# Field Induced Alteration of a Qubit's "Hadamard Time"

Theodosios Geo Douvropoulos

*Hellenic Naval Academy, Physical Sciences Sector, Pure & Applied Physics,*
*Hatzikyriakou Ave. Piraeus, 18539, Greece*
*douvrotheo@yahoo.com*

**Abstract**. In this paper, we explore the dynamics of a qubit state prepared in a double-well potential generated by the coupling of the system with the environment through two independent field barriers. Thus, we adopt the path-integral theory to reveal the system's complex energy spectrum through the construction of its Green's function. In particular, we focus on the alteration of the "Hadamard Time" defined in the current paper. We qualitatively study the aforementioned alteration as a function of various parameters, such as the magnitude of the field barriers, the relative size of the well related to the internal barrier, and the shape similarity factor. We analytically define these quantities inside the manuscript. We also discuss in detail the appearance of the exponential decay rate. Since our results come in analytic form, they permit their future numerical application in realistic physical and quantum computing systems.

**Keywords:** Qubit, Hadamard Gate, Superposition State, Beam Splitter, Double Well Potential (DWP), Path Integral Method, Inversion Period, Exponential Decay Rate, Decoherence

**PACS:** 03.65.−w, 03.65.Sq, 03.65.Xp

## INTRODUCTION

The qubit, which is the quantum version of the classical bit [1], corresponds to a class of quantum systems possessing a characteristic property that can admit two possible values. In general we focus our attention on this property and consider the rest as frozen or out of interest. Thus considering the spin of an electron, the two possible values are namely the spin up and spin down while considering the

polarization of a photon, the horizontal and vertical polarization, [2,3]. As far as the position of an atom or electron is concerned, the double well potential serves as a one dimensional qubit where the atom or electron can be found in the left or right well. Spin qubits can be realized by either solid-state or superconductor technology [4,5], and at the same time position qubits (for instance the presence or absence of an electron in a quantum dot) which are known as charge or electrostatic qubits, can also be implemented either in a semiconductor manner [6,7] or using a Cooper pair box [8,9] in superconductors. A combination of the above deals with the use of hybrid spin-charge superconducting qubits, e.g. transmons, [10]. The interested reader may find a review of the current semiconductor and super-conducting technologies in [11,12].

The one-dimensional double well potential (DWP), depicted by Figure 3 that follows, not only stands throughout the ages as a model for the study of some peculiar but still most basic quantum phenomena, such as internal tunneling and energy splitting, but at the same time is a widely used practical model for the study of a variety of systems and processes in Physical Sciences. Out of the plethora of such studies, we distinguish the Ammonia maser [13,14], the Bose Einstein condensates [15-17], structural phase transitions [18], matter-wave interferometry in atomic dimensions [19], realization of qubits, [20], and realization of beam splitters [21].

Quantum computation strongly relies on the realization, manipulation and control of qubits. As far as the realization is concerned, a basic technique deals with the construction of a double - well potential in such a way that the energies of its first two eigenstates appear to have a large gap with the rest, [22,23]. For example holes in quantum wells have the attractive property of a light effective mass which is highly desirable for spin qubits since it provides large energy level spacing in quantum dots, [24]. In addition it is well known from the late 90s that we can use linear components of quantum optics technology, such as lossless symmetric beam splitters, for the implementation of universal quantum gates such as the Hadamard gate, and to further perform precisely the computation of quantum gates and algorithms, [25]. A Bose Einstein Condensate beam splitter uses condensates instead of single particles and can be realized with a DWP of tunable height, [21].

A single particle qubit implemented as a DWP, can be built up from two coupled semiconductor quantum dots, where the band offset of different materials in one direction results in an effective one dimensional DWP, [26-28]. Alternatively it can be built up through the use of superconductor devices based on the Josephson effect, where the effective DWP results via a RF-SQUID circuit [29-31]. A third option comes from trapped ions in a DWP which are confined via the use of strong magnetic and electric fields, [33-35]. However it is extremely difficult to confine a trapped ion in different topology than the one of a in-line arrangement providing a low scalability and in addition just as other quantum processors they demand extremely low temperatures. Despite the complexity of the above mentioned systems, their basic structure and dynamics can be explained through basic principles of the one dimentional DWP, [35-37].

Thus, during the recent years many different schemes both theoretical and experimental have been proposed for the implementation and manipulation of qubits through effective one dimensional DWP. Mentioning a few we distinguish the analysis of the phase evolution of the Cooper pairs wave function for obtaining a DWP with cusp barriers for current qubits, [38], the DWP Josephson junction between two d-wave superconductors, as an implementation of a phase or flux qubit, [39], the analysis for designing a vortex qubit created in a DWP in a semiannular

Josephson junction, [40,41], buckling nanobars which are nano-electromechanical quantum coherent systems as to be forming a DWP for charge qubits, [42], quantum dots in semiconductor nanocolumns prepared by epitaxial growth and where the carrier confinement  in the direction of the DWP can be achieved by conformal overgrowth of a semiconductor barrier layer, [43], and many others.

A suitably engineered quantum well can stabilize the charge state of the qubit against photoionization [44] and when an electric field is imposed on the DWP the induced lack of inversion symmetry allows the possibility of different qubit manipulation methods such as electron spin resonance, electric dipole spin resonance and g-tensor modulation resonance, [45]. On the other hand the most exotic phenomena of quantum mechanics such as quantum entanglement can be produced through a DWP qubit and its interaction with a source of non classical light, [46]. In addition, single and two-qubit operations can be realised through a high degree of control over the tunnel coupling of the DWP, while spin-orbit coupling obviates the need for microscopic elements and enables rapid qubit control through fast rotations, [47].

As far as the dynamics of the qubit is concerned, decoherence was understood to play a key role at the very beginning of quantum computation, [48]. Coherence time refers to the length of time that a quantum superposition state can survive. The key is to have a quantum superposition live longer than it takes to perform an operation or experiment. Manipupation of the qubic destroys isolation and induces decoherence of its state. It is experimentally observed that spin-based qubits  maintain coherence for a longer time length than electrostatic qubits [49].

Hence, all the above motivated us for producing the current work.  In this paper we study the dynamics, meaning the time evolution, of a qubit state in a DWP, which is a potential that possesses two minima separated by an internal barrier, under the additional influence of a two channel (barrier) field, as this is depicted by Figure 2 that follows. In a way, it continues previous works of ours on the DWP, [50,51]. Such a model adds to the normal dynamics of the DWP the possibility of irreversible dissipation to the free particle continuum. The work described in this paper, constitutes a particular implementation of the path integral method to the model potential which is depicted by Figure 2, where a barrier field is inserted in each side of the unperturbed potential of the qubit, in order to qualitatively describe not only the field-induced variation of energy splitting and/or time period of internal oscillation, but the appearance of exponential decay rates as well, describing the dissociation of the qubit. However we should have in mind, that when it comes to application, most of the formal and mathematical work uses arbitrary parameters. Therefore, the interesting information of such calculations is not in the absolute value of the numbers, since it is hard to see how experimental conditions and measurements can test exactly the model problem. In addition, the present treatment has allowed the derivation of analytic formulas for the energies, the energy shifts, and energy widths, due to tunneling. Such a potential has not been treated before analytically, making the problem rather challenging.

The present paper is organized as follows. In the first section we describe in short the path integral method to be applied, for the construction of the qubit's Green's function, introducing the various phase factors to be used. Next we actually apply the method and gradually construct the qubit's Green's function, by taking in account the various phase factors that the system's topology acquires through successive propagation and reflection events. We also carry out the tedious algebra and calculate the qubit's Green's function in a compact fractional form.  In the third section we

briefly review the dynamics (time evolution) of the DWP and define the Hadamard Time. Next we bring out the significance of its energy spectrum, as far as the energy splitting and the Hadamard Time are concerned. In the fourth section we reveal the system's complex energy spectrum, while in the next section we analyze the dynamics of the model studied, concerning the alteration of the Hadamard Time and the exponential decay rate, for various values of the parameters used. In this section we introduce quantity $sim(\widehat{\xi}, \breve{\vartheta})$ that measures the shape of the qubit's internal barrier relative to the one of its well. In the final section we conclude, and light our most important results.

# THE CONSTRUCTION OF THE QUBIT'S GREEN'S FUNCTION VIA PATH INTEGRALS

As is well known, both the Schrodinger and Heisenberg picture in Quantum Mechanics, deal with the basic dynamical differential equations involving either the states or the operators, [52]. In deep contrast, Feyman's formulation of path integration [53], offers an alternative geometric picture and targets directly towards the solution of the Schrodinger equation, which is constructed in the form of a propagator.

Feynman showed how a system's propagator can be determined by the "sum over histories", meaning quantity

$$K_F = N \int e^{iS(x(t))/\hbar} Dx(t) \tag{1}$$

where the above functional expresses the sum over the classical paths and $S$ stands for the classical action. Thus, the square meter of the propagator, which is $|K(x, t_2 \; ; \; x_1, t_1)|^2$, gives the probability of finding the particle at the time $t_2$, assuming the starting and ending point to be $x_1$ and $x_2$ respectively. Its energy Fourier transform, called the fixed energy amplitude [54], is the system's Green's function $K(E)$. Its construction reveals the energy spectrum of the system under study, since the Green's function can be written as a sum of energy pole terms of the following form

$$K(E) \sim \sum_n \frac{c_n}{E - Z_n} \tag{2}$$

The $Z_n$ energy poles may be real or complex, depending on the dynamics of the system under study.

In their periodic orbit theory, Gutzwiller [56] and later Miller [57,58], showed the way Green's function can be constructed for one dimensional propagation, via the calculation of all the possible changes in phase of the wave-function through the corresponding changes of the action, during the system's propagation over the classical paths. Holstein [59] in his seminal work, put all these together, and nicely showed how the fixed energy amplitude, can be used to achieve analytic continuation

of the propagator to forbidden regions of motion, (potential barriers), where the particle travells in imaginary times. His central result for the calculation of the transmission amplitude via an infinite set of paths that the particle follows, can be written in the compact form that follows

$$K(E) \;=\; \sum_{j=1}^{\infty}\left\{\prod_{i=1}^{N(j)} \frac{m}{\hbar^2 \,_{r_1}k_{r_2}} s_{ij}^{2\pi}\right\} \tag{3}$$

In the above equation $_{r_1}k_{r_2}$ is a non local wave number of the particle connecting the initial and the final point of propagation and defined by

$$_{r_1}k_{r_2} \equiv \sqrt{k(r_1)k(r_2)} \tag{4}$$

where $k(y)=\sqrt{2m(E-V(y))/\hbar^2}$ ,with $E$ standing for the energy and $V(y)$ for the potential function. The index $j$ corresponds to a particular path, while the index $i$ corresponds to a certain event along the path. Therefore, the symbol $s_{ij}^{2\pi}$ represents each $i$ event factor that contributes to the $j^{\text{th}}$ path normalized to the maximum change in phase which is equal to $2\pi$. Their total number is $N(j)$ and depends on the path. These event factors are of two types. One type represents propagation and the other represents reflection from a turning point.

The $s_{ij}^{2\pi}$ propagation event phase factors describe propagation (from a to b) in an either allowed region (given by $\exp\left[i\int_a^b k(y)dy\right]\equiv e^{i\breve{g}(b)} \equiv \breve{g}_b$ , where the $\cup$ superscript stands for the shape of the well), or in a forbidden region (from b to c) of motion (given by $\exp\left[-\left|\int_b^c \lambda(y)dy\right|\right]\equiv e^{-\hat{\xi}(b)}\equiv \hat{\xi}_b$ with $\lambda(y)=\sqrt{2m(V(y)-E)/\hbar^2}=ik(y)$, where the $\cap$ superscript stands for the shape of the barrier). The dimensionless phase quantities $\breve{g}(b)$ and $\hat{\xi}(b)$ will be called the "qubit well magnitude" (qwm) and the " qubit barrier magnitude" (qbm) respectively. A large qwm corresponds to a deep and broad potential well while a large qbm corresponds to a high and broad potential barrier. These quantities appear continuously in the text and figures that follow and play a significant role in the qubit's dynamics since the first contributes to the oscillation of its orthogonal basis states and the second to the tunneling phenomenon. The $s_{ij}^{2\pi}$ reflection event phase factors describe reflections from turning points, ($-i$ for reflection from a turning point in an allowed region, $+i/2$ for reflection in a forbidden region , and $-1$ for reflection from an infinite barrier).

However, someone notes that the reflection factors (except of course for the case of an infinite barrier), do not take in account the relative size of the involved areas. For example if a particle is reflected back to a classically allowed region of motion, the reflection factor will always be equal to (-i), no matter how large is in magnitude the potential barrier on the other side of the turning point. Clearly, this is an issue that has to be solved and it actually does in the context of the present research, as will be seen later. Both $\breve{g}(b)$ and $\hat{\xi}(b)$ are dimensionless phase quantities. The above mentioned rules are in total depicted by Figure 1 that follows and can also be found in standard textbooks of path integrals, or quantum tunneling as well, [54,60]. For the

present requirement of computing the overall transmission amplitude, the points $r_1$ and $r_2$ are in the classically allowed region of motion of the left well of Figure 2.
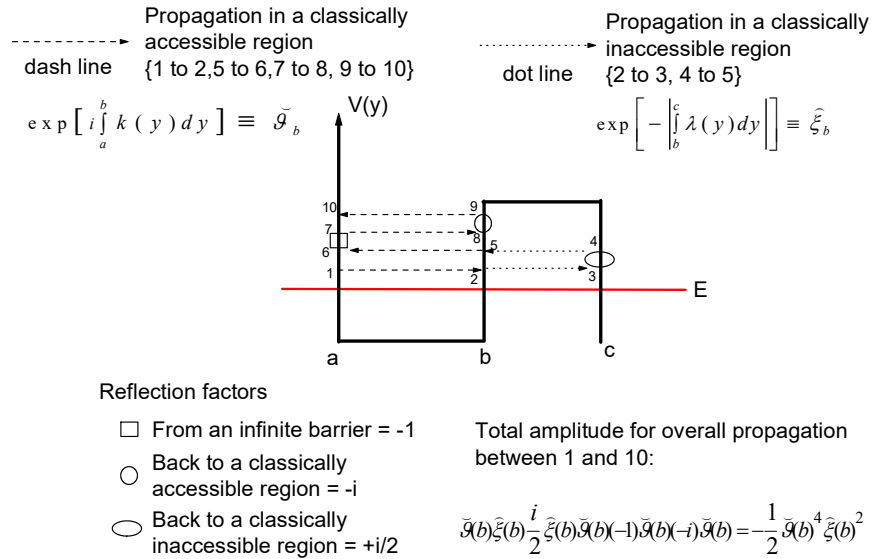


**FIGURE 1.** The rules for the construction of the path integral amplitudes through the $s_{ij}^{2\pi}$ event factors. Here we depict a path example involving 9 event phase factors. The dash line stands for propagation in a classically allowed region, while the dot line for propagation in a classically inaccessible region. These regions are characterised so by the relative value of the energy. The square reflection factor (-1) stands for reflection from an infinite barrier, the circle reflection factor (-i) for reflection back to a classically allowed region and the elliptic reflection factor (+i/2) for reflection back to a classically inaccessible region.

As far as the model is considered to have only one degree of freedom, corresponding to the relative position of the atom or electron, it can be treated as a one dimensional physical system. Thus we can apply the path integral method for the construction of the Green's function. In addition we should sketch the perturbed one dimensional potential as in Figure 2 that follows:
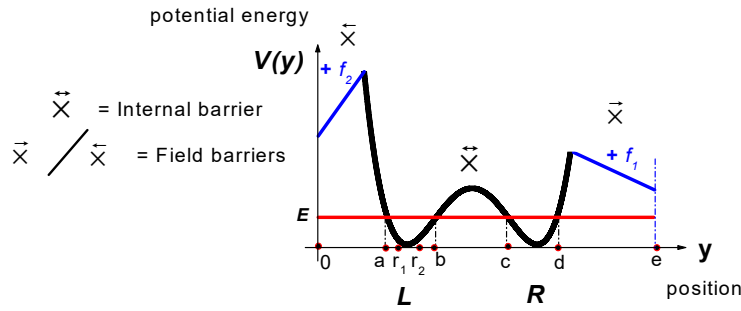
**FIGURE 2.** The potential of a perturbed double well. There are five regions of motion: the classically accessible regions L and R corresponding to states $|0\rangle$ and $|1\rangle$, and the classically inaccessible regions $\overleftrightarrow{\times}$, $\vec{\times}$, $\overleftarrow{\times}$ of the internal and the field barriers respectively. The blue lines $f_1$ and $f_2$ stand for the electrostatic field imposed on the right and left well respectively while $E$ stands for the particle's energy. The slope of $f_1$ and $f_2$ is proportional to the corresponding field strength. There are four turning points of motion (a,b,c,d) and points $r_1$ and $r_2$ lie between a and b of the left well.

Figure 2 describes the induced topology of the potential as this is determined by the specific value of the energy. There are four turning points, meaning a, b, c, and d. In this way we have five regions of motion, two classically allowed (L and R wells) and three classically forbidden (barriers $\overleftrightarrow{\times}$, $\vec{\times}$, $\overleftarrow{\times}$). In order to construct the overall transition amplitude for propagation between points $r_1$ and $r_2$ of region L, we divide the problem into simpler ones.

For this we write $K(E)$ as a sum of transition amplitudes involving specific regions of motion each time, of the form:

$$K(E) = \frac{m}{\hbar^2 k_{r_1 ; r_2}} \left\{ \Upsilon^L + \Upsilon^{L,\vec{\times}} + \Upsilon^{L,\vec{\times},|1\rangle} + \Upsilon^{L,\vec{\times},R,\vec{\times}} + \Upsilon^{L,\vec{\times},R,\vec{\times},\overleftarrow{\times}} \right\} \tag{5}$$

where $\Upsilon^{L,\vec{\times},R}$ for example denotes the amplitude for propagation involving the classically allowed regions L and R as well as the internal barrier, in all possible ways. Table 1 that follows explains the symbols that we will use in the rest of the manuscript, concerning the various amplitudes.

| SYMBOL | DESCRIPTION |
|---|---|
| $\breve{\mathcal{G}}_r$ | Contribution of a single propagation in a classically allowed region as a function of the ending point r for starting point a |
| $\widehat{\xi}_b$ | Contribution of a single propagation in a classically forbidden region as a function of the starting point b |
| $\vec{A}_q(r_1;r_2)$ | Amplitude for a single propagation from left to right inside region q between points $r_1$ and $r_2$ |
| $A_q(r_1;r_2)$ | Amplitude for infinite repetitions of the propagation between $r_1$ and $r_2$ in all possible ways, while staying at region q |
| $\left\{ p \underset{r_1}{\overset{r_2}{\rightleftarrows}} q \right\}$ | Overall amplitude for exhausting combination of the regions p and q propagating between $r_1$ and $r_2$ |
| $\Upsilon^{p,q}$ | Total contribution to the Green's function through the exclusive combination of regions p and q |

**TABLE 1.** Basic symbols and their definition, in the current manuscript.

In Appendix A we separately develop each amplitude of eq.(4) providing the basic steps. In the lines that follow we give an example by calculating the contribution of the L well. Transition Amplitude $\Upsilon^L$ involves propagation inside the classically allowed region of the left potential well where the state $|0\rangle$ lives. It is constructed by fundamental amplitudes, for example $\vec{A}_L(r;a)$ that connects points r and a in a single straight path moving from right to left, (the arrow denotes direction), and by amplitudes $A_L(r;a)$, that connect r and a with infinite repetitions (including reflections) in all possible ways. In this way we can write:

$$\Upsilon^L = \vec{A}_L(r_1;r_2) + \vec{A}_L(r_1;a)(-i)\left\{ A_L(a;a)(-i)\vec{A}_L(a;r_2) + A_L(a;b)(-i)\vec{A}_L(b;r_2) \right\}$$
$$+ \vec{A}_L(r_1;b)(-i)\left\{ A_L(b;b)(-i)\vec{A}_L(b;r_2) + A_L(b;a)(-i)\vec{A}_L(a;r_2) \right\} \tag{6}$$

Table 2 that follows contains the calculation of the above mentioned fundamental amplitudes:

| Fundamental amplitudes of area L | Function of event phase factors |
|---|---|
| $\vec{A}_L(r_1;r_2)$ | $\breve{\vartheta}_{r_2}/\breve{\vartheta}_{r_1}$ |
| $\vec{A}_L(r_1;a)$ | $\breve{\vartheta}_{r_1}$ |
| $\vec{A}_L(r_1;b)$ | $\breve{\vartheta}_b/\breve{\vartheta}_{r_1}$ |
| $\vec{A}_L(a;r_2)$ | $\breve{\vartheta}_{r_2}$ |
| $\vec{A}_L(b;r_2)$ | $\breve{\vartheta}_b/\breve{\vartheta}_{r_2}$ |
| $A_L(a;a)$ | $\left\{2\,\mathrm{Re}\left(\breve{\vartheta}_b\right)\breve{\vartheta}_b\right\}^{-1}$ |
| $A_L(a;b)$ | $\left\{2\,\mathrm{Re}\left(\breve{\vartheta}_b\right)\right\}^{-1}$ |

**TABLE 2.** Calculation of the amplitudes involved in the propagation inside region L.

Giving a second example, the $A_L(a;a)$ amplitude comes from the infinite repetition of the $(a;a)$ propagation, including the reflection factors, which is

$$A_L(a;a) = 1 + \breve{\vartheta}_b(-i)\breve{\vartheta}_b(-i) + \dots = \frac{1}{1+\breve{\vartheta}_b{}^2} = \frac{1}{2\breve{\vartheta}_b\,\mathrm{Re}\,\breve{\vartheta}_b} \tag{7}$$

It is also clear that

$$A_L(a;b) = \breve{\vartheta}_b A_L(a;a) = \frac{1}{2\,\mathrm{Re}\,\breve{\vartheta}_b} \tag{8}$$

Putting all these together we get for the $\Upsilon^L$ amplitude the following expression

$$\Upsilon^L = \breve{\vartheta}_{r_2}/\breve{\vartheta}_{r_1} + \frac{1}{1+\breve{\vartheta}_b{}^2}\left\{-i\frac{\breve{\vartheta}_b{}^2}{\breve{\vartheta}_{r_2}\breve{\vartheta}_{r_1}} - \breve{\vartheta}_b{}^2\frac{\breve{\vartheta}_{r_1}}{\breve{\vartheta}_{r_2}} - i\breve{\vartheta}_{r_2}\breve{\vartheta}_{r_1}\right\} \tag{9}$$

Introducing $\breve{\vartheta}_b{}^{\pi/4} = i^{1/2}\breve{\vartheta}_b$ we finally get for the $\Upsilon^L$ amplitude

$$\Upsilon^L = -2i\frac{\mathrm{Im}\,\breve{\vartheta}_{r_1}^{\pi/4}}{\breve{\vartheta}_{r_2}^{\pi/4}} + \frac{2\,\mathrm{Im}\,\breve{\vartheta}_{r_1}^{\pi/4}\,\mathrm{Im}\,\breve{\vartheta}_{r_2}^{\pi/4}}{\breve{\vartheta}_b\,\mathrm{Re}\,\breve{\vartheta}_b} \tag{10}$$

Equation A.15 of Appendix A gives Green's function for the total amplitude contribution, as

$$K(E) = \frac{m}{\hbar^2 k_{r_1;r_2}}\left\{\frac{1}{2\left\{1-\Upsilon^{L+\vec{x}+R+\vec{x}}(r_1;a)A_{\vec{x}}(a;a)\right\}\breve{\vartheta}_b\,\mathrm{Re}\,\breve{\vartheta}_b}\right\} \tag{11}$$

where the amplitude $\Upsilon^{L+\vec{x}+R+\vec{x}}$ is defined by equation A.12 of Appendix A and given as

$$\Upsilon^{L+\vec{\times}+R+\vec{\times}} = -2i\frac{\mathrm{Im}\,\breve{\vartheta}^{\pi/4}_{r_1}}{\breve{\vartheta}^{\pi/4}_{r_2}} +$$

$$2\frac{\mathrm{Im}\,\breve{\vartheta}^{\pi/4}_{r_1}\,\mathrm{Im}\,\breve{\vartheta}^{\pi/4}_{r_2}}{\breve{\vartheta}_b}\,\frac{1}{4\,\mathrm{Re}\,\breve{\vartheta}_b - \breve{\xi}_b{}^2\breve{\vartheta}_b \pm \dfrac{\left\{-4\breve{\xi}_b{}^2\breve{\vartheta}_b{}^4 + \dfrac{\left(4\breve{\xi}_b\hat{\gamma}_d\right)^2\breve{\vartheta}_b{}^3\,\mathrm{Re}\,\breve{\vartheta}_b}{\left(4\,\mathrm{Re}\,\breve{\vartheta}_b - \breve{\xi}_b{}^2\breve{\vartheta}_b\right)^2 + \left(\breve{\xi}_b\hat{\gamma}_d\right)^2}\right\}^{1/2}}{\breve{\vartheta}_b}} \qquad (12)$$

and the field barriers $\vec{\times}$ and $\bar{\times}$ acquire phase factors to form the following barrier magnitudes $\exp\left[-\left|\int_d^e\tau(y)dy\right|\right]\equiv e^{-\gamma(d)}\equiv\hat{\gamma}_d$ and $\exp\left[-\left|\int_0^a\tau(y)dy\right|\right]\equiv e^{-\delta(a)}\equiv\hat{\delta}_a$

respectively, and where of course $A_{\bar{\times}}(a;a)=\dfrac{i}{2}\dfrac{\hat{\delta}_a{}^2}{1+\hat{\delta}_a{}^2/4}$ .

## SHORT REVIEW OF THE TIME EVOLUTION OF A QUANTUM STATE IN A DOUBLE WELL POTENTIAL

In the present chapter we briefly review the dynamics concerning the time evolution of a quantum state in a double well structure, as this can be found in any standard textbook of quantum mechanics and quantum tunneling [14,61]. For this, we assume to have the two initially separated lowest, degenerate eigenstates of the two independent unperturbed wells, namely $|0\rangle$ and $|1\rangle$ with energy $E_o$, that do not overlap with each other, as depicted by Figure 3 that follows. These states will interact through the finite potential barrier that separates the two wells to construct the eigenfunctions of the DWP. Since the potential is an even function, its Hamiltonian commutes with the parity operator. Thus we can construct an orthonormal basis of symmetric and antisymmetric states, as follows

$$S = \frac{1}{\sqrt{2}}\{|0\rangle + |1\rangle\} \quad \text{and} \quad A = \frac{1}{\sqrt{2}}\{|0\rangle - |1\rangle\} \qquad (13)$$

In fact we can mathematically describe the finite potential barrier as a perturbation matrix of the form $U = -\delta\sigma_\times$, [62], where of course $\sigma_\times$ stands for the Pauli matrice:

$$\sigma_\times = \begin{pmatrix} 0 & 1 \\ 1 & 0 \end{pmatrix} \qquad (14)$$

Hence the total Hamiltonian becomes equal to $H = \begin{pmatrix} E_o & -\delta \\ \delta & E_o \end{pmatrix}$. Diagonalization of the Hamiltonian gives two new eigenvalues for the symmetric and antisymmetric state, which are respectively: $E_S = E_o - \delta$ and $E_A = E_o + \delta$, whose energy distance is equal to $\varDelta = 2\delta$. Thus, the degeneration of the two initial states is removed, and an energy splitting appears of the corresponding energy levels.

Let us assume now that at $t=0$ the system is prepared in the state $|0\rangle$ of the left well, which can be written as a superposition of states of the DWP:

$\Psi(t=0) = |0\rangle = \dfrac{1}{\sqrt{2}}\{S + A\}$. The time evolution of the state will then be

$\Psi(t) = \dfrac{1}{\sqrt{2}}\left\{e^{-it(E_o-\delta)/\hbar}S + e^{-it(E_o+\delta)/\hbar}A\right\}$. In terms of the initial eigenfunctions of the two separate wells, we can write

$$\Psi(t) = e^{-itE_o/\hbar}\left\{\cos(\delta t/\hbar)|0\rangle + i\sin(\delta t/\hbar)|1\rangle\right\} \qquad (15)$$

We particularly focus on the "Hadamard Time", defined as the time needed for the initial state of the qubit ($|0\rangle$ or $|1\rangle$) to come in an equally weighted superposition of the two complementary orthogonal states, $|0\rangle$ and $|1\rangle$. In the context of the present research activity this time is defined as the Hadamard Time, since the action of the Hadamard gate on $|0\rangle$ is actually $H|0\rangle = \dfrac{1}{\sqrt{2}}\{|0\rangle + |1\rangle\}$. Thus, the time needed for the initial state $|0\rangle$ to come in an equally weighted superposition of itself and its complementary state $|1\rangle$ is equal to

$$T_{Hd} = \dfrac{h}{4\Delta} \qquad (16)$$

Hadamard Time comes as a function of the energy difference of the two lower states of the DWP. Thus, in order to explore the system's dynamics under the action of the two field barriers, we must first analyze its energy spectrum. The diffusion of the initial state to the continuum set of states through the field barriers, turns the spectrum into complex. Hence, the real part of the spectrum determines the alteration of the Hadamard Time while the imaginary part determines the state's decay rate to the continuum, meaning decoherence.
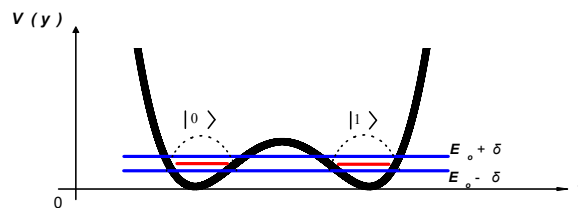


**FIGURE 3.** The doublet splitting in a DWP. The two initially degenerate states $|0\rangle$ and $|1\rangle$ with energy $E_o$ of the two separate unperturbed wells, interact through the internal potential barrier $\tilde{x}$ and form the symmetric (S) and antisymmetric states (A) of the full potential, with energies $E_o - \delta$ and $E_o + \delta$ respectively.

# THE ENERGY SPECTRUM OF THE FIELD PERTURBED DOUBLE WELL

As we have already seen, the step by step construction of the total Green's function, reveals gradually additional fractional pole terms, coming as the extra contribution of each new region of motion. In turn, these poles correspond to the energies of the system due to the qubit interaction with the field barriers.

Thus, for each fractional contribution of the total Green's function, we need to expand the denominator around the eigenvalues $E_n$ of the unperturbed well. In this way, we calculate the energy shift that takes place, coming from both type of barriers, namely the internal qubit and the field diffusion barriers. In Appendix B we analytically calculate the energy poles that arise through the above described method. In the lines that follow we give an example of such calculation, concerning the poles of the unperturbed quantum well meaning region L.

Region L contributes with the pole term:

$$Pole_n^{\ L} \sim \left\{ \breve{\mathcal{G}}_{b,n} \operatorname{Re} \breve{\mathcal{G}}_{b,n} \right\}^{-1} \tag{17}$$

The poles of the fractional term arise naturally from the condition $\operatorname{Re} \breve{\mathcal{G}}_b = 0$, which can be equivalently written as

$$\int_a^b k(y)dy = n\pi + \pi/2 \tag{18}$$

Assuming a parabolic type of potential well, as depicted by Figure 2, meaning a function of the form $V(y) = \kappa(y - y_o)^2$, where $\kappa = \dfrac{2m\pi^2}{T^2}$ with T being the period of classical oscillations and $y_o$ corresponds to the bottom of the well, we can actually calculate the integral in (18) and find the energy poles as

$$E_n = \left( n + \frac{1}{2} \right) \hbar \omega \tag{19}$$

which are the exact eigenvalues of the harmonic potential. Giving another example we can assume a rectangular potential well of infinite walls, which is approximately true as long as we can assure that the internal barrier is much higher than the lower eigenstate of the well. Then we would have instead of (10) the following:

$$\Upsilon^L = -2i \frac{\operatorname{Im} \breve{\mathcal{G}}_{r_1}^{\pi/4}}{\breve{\mathcal{G}}_{r_2}^{\pi/4}} + \frac{2 \operatorname{Im} \breve{\mathcal{G}}_{r_1}^{\pi/4} \operatorname{Im} \breve{\mathcal{G}}_{r_2}^{\pi/4}}{\breve{\mathcal{G}}_b \operatorname{Im} \breve{\mathcal{G}}_b} \tag{20}$$

and consequently

$$\int_a^b k(y)dy = n\pi \Rightarrow \frac{\sqrt{2m}}{\hbar^2}\int_a^b \sqrt{E_n}\,dy = n\pi \Rightarrow E_n = n^2 \frac{\pi^2\hbar^2}{2m(b-a)^2} \tag{21}$$

which of course are the exact eigenvalues of a particle in a box. Thus, the pole term of (17) reveals the eigenvalues of the isolated unperturbed potential well.

According to Appendix B the energy eigenalues for the rest region amplitudes go as following:

a) Regions L and $\breve{\times}$ contribute with the perturbed eigenvalues

$$Z_n^{L,\breve{\times}} = E_n - \hat{\xi}_{b,n}^{\ 2}\left\{d^{E_n}\hat{\xi}(b)\right\}\left(2\sqrt{2}\left\{d^{E_n}\breve{\vartheta}(b)\right\}\right)^{-2} - i\left(d^{E_n}\breve{\vartheta}(b)\right)^{-1}\frac{\hat{\xi}_{b,n}^{\ 2}}{4} \tag{22}$$

where the subscript $n$ denotes calculation on the eigenvalue $E_n$ and where the symbol $d^{E_n}$ denotes derivation with respect to the eigenvalue $E_n$.

b) Regions L, $\breve{\times}$ and R contribute with the perturbed eigenvalues

$$Z_n^{L,\breve{\times},R} = E_n - \frac{\left[\mp\dfrac{\hat{\xi}_{b,n}}{2}\left\{-\left\{d^{E_n}\breve{\vartheta}(b)\right\}\left(1-\dfrac{\hat{\xi}_{b,n}^{\ 2}}{4}\right)\pm\left\{d^{E_n}\hat{\xi}(b)\right\}\dfrac{\hat{\xi}_{b,n}}{2}\right\} \atop -i\dfrac{\hat{\xi}_{b,n}}{2}\left\{-\left\{d^{E_n}\breve{\vartheta}(b)\right\}\dfrac{\hat{\xi}_{b,n}}{2}\left(1-\dfrac{\hat{\xi}_{b,n}^{\ 2}}{4}\right)\pm\left\{d^{E_n}\hat{\xi}(b)\right\}\dfrac{\hat{\xi}_{b,n}^{\ 2}}{4}+\left\{d^{E_n}\hat{\xi}(b)\right\}\hat{\xi}_{b,n}^{\ 2}\mp\left(\left\{d^{E_n}\breve{\vartheta}(b)\right\}\right)\right\}\right]}{\left\{-\left\{d^{E_n}\breve{\vartheta}(b)\right\}\left(1-\dfrac{\hat{\xi}_{b,n}^{\ 2}}{4}\right)\pm\left\{d^{E_n}\hat{\xi}(b)\right\}\dfrac{\hat{\xi}_{b,n}}{2}\right\}^2+\dfrac{\hat{\xi}_{b,n}}{2}\left\{\left\{d^{E_n}\hat{\xi}(b)\right\}\hat{\xi}_{b,n}\mp\left(\left\{d^{E_n}\breve{\vartheta}(b)\right\}\right)\right\}^2} \tag{23}$$

c) Regions $L, \breve{\times}, R, \breve{\times}$ contribute with the perturbed eigenvalues

$$Z_n^{L,\breve{\times},R,\breve{\times}} = E_n - \frac{\left\{\mp 2\hat{\xi}_{b,n}\left\{\left\{d^{E_n}\breve{\vartheta}(b)\right\}\left(4-\hat{\xi}_{b,n}^{\ 2}\right)\pm 2\hat{\xi}_{b,n}^{\ 2}\left\{d^{E_n}\hat{\xi}(b)\right\}\right\}+2\hat{\xi}_{b,n}^{\ 4}\left(\left\{d^{E_n}\hat{\xi}(b)\right\}\mp\hat{\xi}_{b,n}\left\{d^{E_n}\breve{\vartheta}(b)\right\}-2\dfrac{\left\{d^{E_n}\breve{\vartheta}(b)\right\}\hat{\gamma}_{d,n}^{\ 2}}{\left(\hat{\gamma}_{d,n}\hat{\xi}_{b,n}\right)^2-\hat{\xi}_{b,n}^{\ 4}}\right)\right\}}{\left\{\left\{d^{E_n}\breve{\vartheta}(b)\right\}\left(4-\hat{\xi}_{b,n}^{\ 2}\right)\pm 2\hat{\xi}_{b,n}\left\{d^{E_n}\hat{\xi}(b)\right\}\right\}^2+\left\{2\hat{\xi}_{b,n}^{\ 2}\left(\left\{d^{E_n}\hat{\xi}(b)\right\}\mp\hat{\xi}_{b,n}^{-1}\left\{d^{E_n}\breve{\vartheta}(b)\right\}-2\dfrac{\left\{d^{E_n}\breve{\vartheta}(b)\right\}\hat{\gamma}_{d,n}^{\ 2}}{\left(\hat{\gamma}_{d,n}\hat{\xi}_{b,n}\right)^2-\hat{\xi}_{b,n}^{\ 4}}\right)\right\}^2}$$

$$+i\frac{\left\{\mp 4\hat{\xi}_{b,n}^{\ 3}\left(\dfrac{1}{2}\left\{d^{E_n}\hat{\xi}(b)\right\}\mp\dfrac{\hat{\xi}_{b,n}}{4}\left\{d^{E_n}\breve{\vartheta}(b)\right\}\pm\left\{d^{E_n}\breve{\vartheta}(b)\right\}\dfrac{\hat{\gamma}_{d,n}^{\ 2}\hat{\xi}_{b,n}^{-1}}{\hat{\gamma}_{d,n}^{\ 2}-\hat{\xi}_{b,n}^{\ 2}}\right)\right\}}{\left\{\left\{d^{E_n}\breve{\vartheta}(b)\right\}\left(4-\hat{\xi}_{b,n}^{\ 2}\right)\pm 2\hat{\xi}_{b,n}\left\{d^{E_n}\hat{\xi}(b)\right\}\right\}^2+\left\{2\hat{\xi}_{b,n}^{\ 2}\left(\left\{d^{E_n}\hat{\xi}(b)\right\}\mp\hat{\xi}_{b,n}^{-1}\left\{d^{E_n}\breve{\vartheta}(b)\right\}-2\dfrac{\left\{d^{E_n}\breve{\vartheta}(b)\right\}\hat{\gamma}_{d,n}^{\ 2}}{\left(\hat{\gamma}_{d,n}\hat{\xi}_{b,n}\right)^2-\hat{\xi}_{b,n}^{\ 4}}\right)\right\}^2}$$

$$\tag{24}$$

d) finally regions $L, \vec{\times}, R, \vec{\times}$ and $\overleftrightarrow{\times}$ contribute with the perturbed eigenvalues

$$Z_n^{L,\vec{\times},R,\vec{\times},\overleftrightarrow{\times}} = E_n - \frac{\left\{\left(\mp 2\widehat{\xi}_{b,n} - \frac{\widehat{\delta}_{a,n}^2}{4}\right)\left\{\left\{d^{E_n}\bar{\vartheta}(b)\right\}\left(4 + \widehat{\xi}_{b,n}^2 - \frac{\widehat{\delta}_{a,n}^2}{4}\right) - \frac{\widehat{\delta}_{a,n}^2}{2}\left\{d^{E_n}\widehat{\delta}(a)\right\} \pm 2\widehat{\xi}_{b,n}\left\{d^{E_n}\widehat{\xi}(b)\right\}\right\} + \left(-2\widehat{\xi}_{b,n}^2 - \frac{\widehat{\delta}_{a,n}^2}{4}\right)\left\{2\widehat{\xi}_{b,n}^2\left(\left\{d^{E_n}\widehat{\xi}(b)\right\} \mp \widehat{\xi}_{b,n}^{-1}\left\{d^{E_n}\bar{\vartheta}(b)\right\} \pm 2\left\{d^{E_n}\bar{\vartheta}(b)\right\}\frac{\widehat{\xi}_{b,n}^{-1}\widehat{\gamma}_{d,n}^2}{\widehat{\gamma}_{d,n}^2 - \widehat{\xi}_{b,n}^2}\right) - \frac{\widehat{\delta}_{a,n}^2}{2}\left(\frac{1}{2}\left\{d^{E_n}\bar{\vartheta}(b)\right\} + \left\{d^{E_n}\widehat{\delta}(a)\right\}\right)\right\}\right\}}{\left\{\left\{d^{E_n}\bar{\vartheta}(b)\right\}\left(-4 + \widehat{\xi}_{b,n}^2 - \frac{\widehat{\delta}_{a,n}^2}{4}\right) \pm 2\widehat{\xi}_{b,n}\left\{d^{E_n}\widehat{\xi}(b)\right\} - \frac{\widehat{\delta}_{a,n}^2}{2}\left\{d^{E_n}\widehat{\delta}(a)\right\}\right\}^2 + \left\{2\widehat{\xi}_{b,n}^2\left(\left\{d^{E_n}\widehat{\xi}(b)\right\} \mp \widehat{\xi}_{b,n}^{-1}\left\{d^{E_n}\bar{\vartheta}(b)\right\} \pm 2\left\{d^{E_n}\bar{\vartheta}(b)\right\}\frac{\widehat{\xi}_{b,n}^{-1}\widehat{\gamma}_{d,n}^2}{\widehat{\gamma}_{d,n}^2 - \widehat{\xi}_{b,n}^2}\right) - \frac{\widehat{\delta}_{a,n}^2}{2}\left(\frac{1}{2}\left\{d^{E_n}\bar{\vartheta}(b)\right\} + \left\{d^{E_n}\widehat{\delta}(a)\right\}\right)\right\}^2}$$

$$+ i \frac{\left\{\left(\mp 2e^{-\phi(\lambda_n)} - \frac{e^{-2\delta_n(\kappa)}}{4}\right)\left\{2e^{-2\phi_n(\lambda)}\left(\left\{d^{E_n}\widehat{\xi}(b)\right\} \mp e^{\phi_n(\lambda)}\left\{d^{E_n}\bar{\vartheta}(b)\right\} \pm 2\left\{d^{E_n}\bar{\vartheta}(b)\right\}\frac{e^{-2\gamma_n(\nu)+\phi_n(\lambda)}}{e^{-2\gamma_n(\nu)} - e^{-2\phi_n(\lambda)}}\right) - \frac{\widehat{\delta}_{a,n}^2}{2}\left(\frac{1}{2}\left\{d^{E_n}\bar{\vartheta}(b)\right\} + \left\{d^{E_n}\widehat{\delta}(a)\right\}\right)\right\} + \left(e^{-\phi(\lambda_n)} + \frac{\widehat{\delta}_{a,n}^2}{4}\right)\left\{\left\{d^{E_n}\bar{\vartheta}(b)\right\}\left(-4 + \widehat{\xi}_{b,n}^2 - \frac{\widehat{\delta}_{a,n}^2}{4}\right) \pm 2e^{-\phi_n(\lambda)}\left\{d^{E_n}\widehat{\xi}(b)\right\} - \frac{\widehat{\delta}_{a,n}^2}{2}\left\{d^{E_n}\widehat{\delta}(a)\right\}\right\}\right\}}{\left\{\left\{d^{E_n}\bar{\vartheta}(b)\right\}\left(-4 + \widehat{\xi}_{b,n}^2 - \frac{\widehat{\delta}_{a,n}^2}{4}\right) \pm 2\widehat{\xi}_{b,n}\left\{d^{E_n}\widehat{\xi}(b)\right\} - \frac{\widehat{\delta}_{a,n}^2}{2}\left\{d^{E_n}\widehat{\delta}(a)\right\}\right\}^2 + \left\{2\widehat{\xi}_{b,n}^2\left(\left\{d^{E_n}\widehat{\xi}(b)\right\} \mp \widehat{\xi}_{b,n}^{-1}\left\{d^{E_n}\bar{\vartheta}(b)\right\} \pm 2\left\{d^{E_n}\bar{\vartheta}(b)\right\}\frac{\widehat{\xi}_{b,n}^{-1}\widehat{\gamma}_{d,n}^2}{\widehat{\gamma}_{d,n}^2 - \widehat{\xi}_{b,n}^2}\right) - \frac{\widehat{\delta}_{a,n}^2}{2}\left(\frac{1}{2}\left\{d^{E_n}\bar{\vartheta}(b)\right\} + \left\{d^{E_n}\widehat{\delta}(a)\right\}\right)\right\}^2}$$

(25)

# FIELD INDUCED DYNAMICS OF A QUBIT STATE

The time evolution of a qubit state in a double well structure, as this is induced by the presence of two independent field barriers depicted by Figure 2, concerns the alteration of the Hadamard Time, as well as the appearance of the exponential decay of the initial state into the continuum. As we have already seen the spectrum turns to be complex taking the following form for the lowest state: $E_o + \delta E_O - i\frac{\Gamma_o}{2}$. As far as the real part is concerned, the result is the splitting of the $E_o$ which is the lowest energy of the unperturbed wells, into two new states, with energies equal to

$$E_S = E_o + \delta E_o^s , \qquad E_A = E_o + \delta E_o^a \tag{26}$$

and then the Hadamard Time is given according to (16) as

$$T_{Hd/f} = \frac{h}{4\left(\delta E_o^a - \delta E_o^s\right)} \tag{27}$$

where the subscript $f$ generally denotes the presence of a field barrier.
In the absence of the field barriers the WKB approximation is obtained as [24,26]

$$T_{Hd/WKB} = \frac{\pi^2}{2\omega\widehat{\xi}_{b,o}} \tag{28}$$

where $\omega$ is the frequency of the classical periodic motion between turning points a and $b$ corresponding to energy $E_O$. The above result in (26) is obtained using the linear connection formulae. In the lines that follow we calculate the Hadamard Time separately for the cases of i) the unperturbed DWP, ii) the double well plus field barrier $f_1$ and iii) the double well plus both field barriers $+ f_1$ and $+f_2$ depicted by Figure 2.

   i)      The case of the Unperturbed Double Well Potential:

According to (23) the real parts of the doublet splitting, read

$$E_o^{L,\breve{x},R} = E_o - \frac{\mp\frac{\widehat{\xi}_{b,o}}{2}\left\{-\left\{d^{E_o}\breve{g}(b)\right\}\left(1-\frac{\widehat{\xi}_{b,o}^2}{4}\right)\pm\left\{d^{E_o}\widehat{\xi}(b)\right\}\frac{\widehat{\xi}_{b,o}}{2}\right\}}{\left\{-\left\{d^{E_o}\breve{g}(b)\right\}\left(1-\frac{\widehat{\xi}_{b,o}^2}{4}\right)\pm\left\{d^{E_o}\widehat{\xi}(b)\right\}\frac{\widehat{\xi}_{b,o}}{2}\right\}^2 + \frac{\widehat{\xi}_{b,o}}{2}\left\{\left\{d^{E_o}\widehat{\xi}(b)\right\}\widehat{\xi}_{b,o}\mp\left(\left\{d^{E_o}\breve{g}(b)\right\}\right)\right\}^2} \tag{29}$$

Thus the Hadamard Time is given as:

$$T_{Hd}^{L,\breve{x},R} = T_{Hd/WKB}\left\{\frac{\frac{1}{2}\left\{\left(1-\frac{\widehat{\xi}_{b,o}^2}{4}\right)-sim(\widehat{\xi},\breve{g})\frac{\widehat{\xi}_{b,o}}{2}\right\}}{\left\{\left(1-\frac{\widehat{\xi}_{b,o}^2}{4}\right)+sim(\widehat{\xi},\breve{g})\frac{\widehat{\xi}_{b,o}}{2}\right\}^2 + \frac{\widehat{\xi}_{b,o}}{2}\left\{sim(\widehat{\xi},\breve{g})\widehat{\xi}_{b,o}+1\right\}^2} + \frac{\frac{1}{2}\left\{\left(1-\frac{\widehat{\xi}_{b,o}^2}{4}\right)+sim(\widehat{\xi},\breve{g})\frac{\widehat{\xi}_{b,o}}{2}\right\}}{\left\{\left(1-\frac{\widehat{\xi}_{b,o}^2}{4}\right)-sim(\widehat{\xi},\breve{g})\frac{\widehat{\xi}_{b,o}}{2}\right\}^2 + \frac{\widehat{\xi}_{b,o}}{2}\left\{sim(\widehat{\xi},\breve{g})\widehat{\xi}_{b,o}-1\right\}^2}\right\}^{-1} \tag{30}$$

which of course goes far beyond the WKB expression. In fact, as can clearly be seen, eq. (30) reduces to (28) by keeping only the dominant terms (omitting terms like $e^{-2\phi_o(\lambda)}$ or smaller), and taking the barrier to be energy independent, meaning taking $\left\{d^{E_o}\widehat{\xi}(b)\right\}=0$, for a small energy area around $E_o$ where the splitting takes place.

Thus we are motivated to further explore the energy dependence of the Hadamard Time. For this, we introduced in (30) quantity

$$\left\{ d^{E_o}\widehat{\xi}(b) \right\} / \left\{ d^{E_o}\breve{\vartheta}(b) \right\} \equiv sim(\widehat{\xi},\breve{\vartheta}) \tag{31}$$

defined as the "shape similarity factor" between the barrier and the well, given as the ratio of the change in barrier magnitude to the change in well magnitude, as energy increases, some kind of $\widehat{\xi}(b)$ derivative with respect to $\breve{\vartheta}(b)$. It is easily understood that the above quantity is negative since $\breve{\vartheta}(b)$ increases with the increment of the energy while $\widehat{\xi}(b)$ decreases. The above are depicted by Figure 4 that follows.
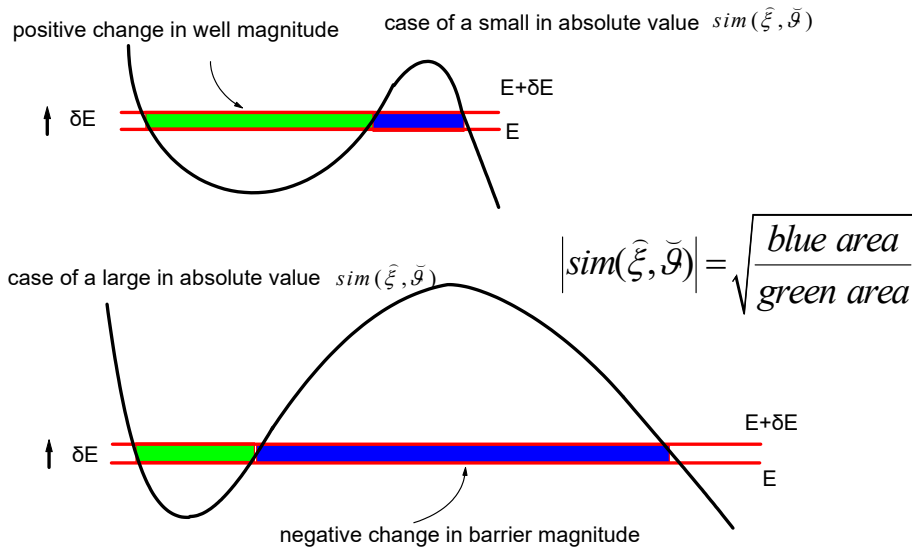


**FIGURE 4.** The variation of the shape similarity factor $sim(\widehat{\xi},\breve{\vartheta})$ for two different cases of the potential barrier shape, relative to the one of the potential well. Note that the blue colour  denotes a negative change in the barrier magnitude as energy increases (shorter barrier) while the green colour a positive change in the well magnitude (deeper well).

In Figure 5 that follows we depict Hadamard Time as a function of the similarity factor for two different values of the qubit barrier, employing (30).
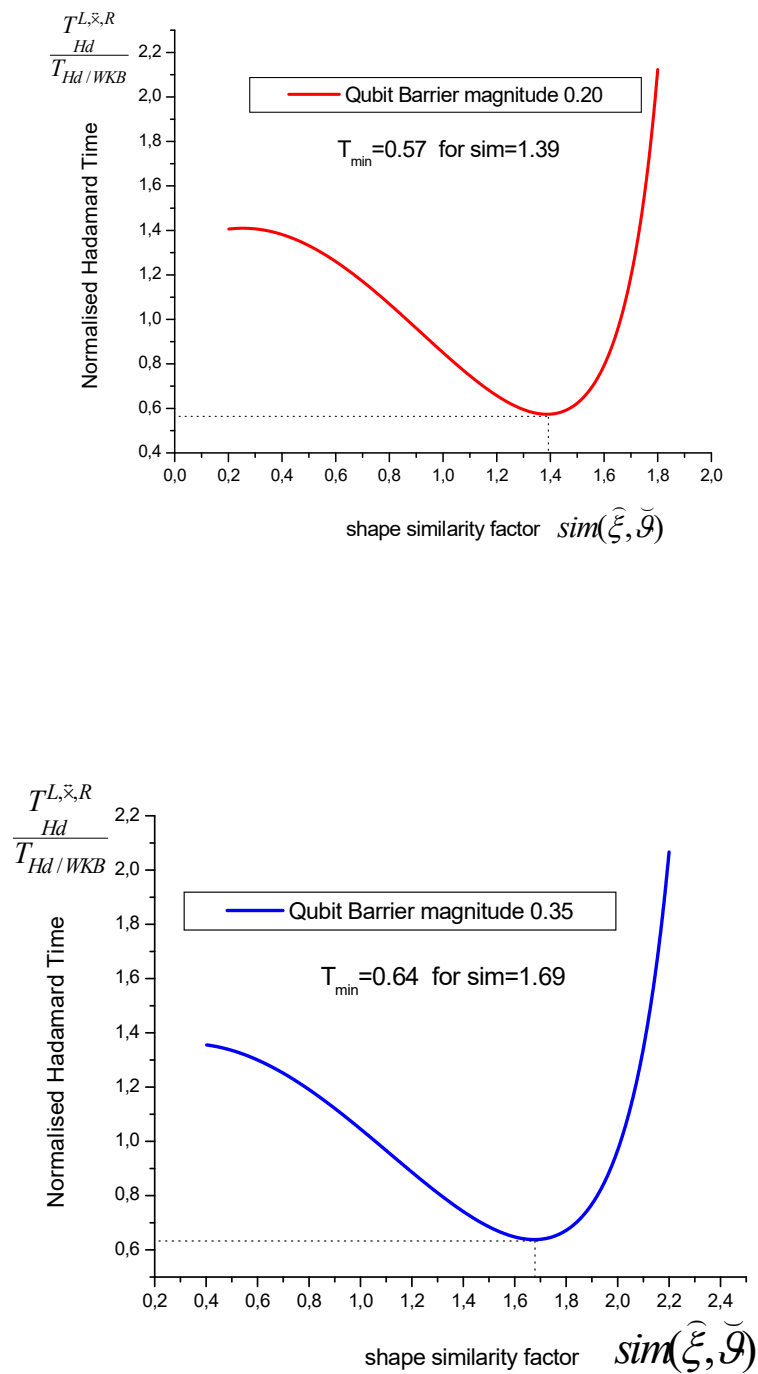
**FIGURE 5.** The variation of the Hadamard Time, (normalised to the WKB expression), as a function of the similarity factor $sim(\widehat{\xi}, \breve{\vartheta})$ which relates the change of the field magnitude to the change of the well magnitude with energy increament, for two different values of the qubit barrier magnitude. For each case the Hadamard Time becomes minimum for a certain value of the similarity factor $sim(\widehat{\xi}, \breve{\vartheta})$.

ii) Field barrier $f_1$ active and field barrier $f_2$ inactive

According to (B-9) of Appendix B the real parts of the energy splitting, read

$$
E_o^{L,\bar{x},R,\bar{x}} = E_o - \cfrac{\left\{\mp 2\hat{\xi}_{b,o}\left\{\left\{d^{E_o}\breve{\mathcal{G}}(b)\right\}\left(4-\hat{\xi}_{b,o}{}^2\right)\pm 2\hat{\xi}_{b,0}\left\{d^{E_o}\hat{\xi}(b)\right\}\right\}+2\hat{\xi}_{b,o}{}^4\left(\left\{d^{E_o}\hat{\xi}(b)\right\}\mp\hat{\xi}_{b,o}\left\{d^{E_o}\breve{\mathcal{G}}(b)\right\}-2\cfrac{\left\{d^{E_o}\breve{\mathcal{G}}(b)\right\}\hat{\gamma}_{d,o}{}^2}{\left(\hat{\gamma}_{d,o}\hat{\xi}_{b,o}\right)^2-\hat{\xi}_{b,o}{}^4}\right)\right\}}{\left\{\left\{d^{E_o}\breve{\mathcal{G}}(b)\right\}\left(4-\hat{\xi}_{b,o}{}^2\right)\pm 2\hat{\xi}_{b,0}\left\{d^{E_o}\hat{\xi}(b)\right\}\right\}^2+\left\{2\hat{\xi}_{b,o}{}^2\left(\left\{d^{E_o}\hat{\xi}(b)\right\}\mp\hat{\xi}_{b,o}{}^{-1}\left\{d^{E_o}\breve{\mathcal{G}}(b)\right\}-2\cfrac{\left\{d^{E_o}\breve{\mathcal{G}}(b)\right\}\hat{\gamma}_{d,o}{}^2}{\left(\hat{\gamma}_{d,o}\hat{\xi}_{b,o}\right)^2-\hat{\xi}_{b,o}{}^4}\right)\right\}^2}
$$

(32)

For the present purpose we currently disregard the energy dependence of the field barrier and write the real parts of the energy splitting as follows

$$
E_o^{L,\bar{x},R,\bar{x}} = E_o - \cfrac{\left\{\mp 8\hat{\xi}_{b,o}\mp 2\hat{\xi}_{b,o}{}^3-4\left(\cfrac{\hat{\gamma}_{d,o}{}^2}{\hat{\gamma}_{d,o}{}^2\hat{\xi}_{b,o}{}^{-2}-1}\right)\right\}}{\left\{16\left\{d^{E_o}\breve{\mathcal{G}}(b)\right\}\right\}\left\{1+\left(\cfrac{\hat{\gamma}_{d,o}{}^2}{\hat{\gamma}_{d,o}{}^2-\hat{\xi}_{b,o}{}^2}\right)^2\right\}}
$$

(33)

Thus the Hadamard Time is given as:

$$
T_{Hd}^{f_1} = T_{Hd/WKB}\left(1+\frac{\hat{\xi}_{b,o}{}^2}{4}\right)^{-1}\left\{1+\left(\frac{\hat{\gamma}_{d,o}{}^2}{\hat{\gamma}_{d,o}{}^2-\hat{\xi}_{b,o}{}^2}\right)^2\right\} \Rightarrow
$$

$$
\frac{T_{Hd}^{f_1}}{T_{Hd/WKB}} = \left(1+\frac{\hat{\xi}_{b,o}{}^2}{4}\right)^{-1}\left\{1+\left(\frac{e^{-2\delta m}}{e^{-2\delta m}-1}\right)^2\right\}
$$

(34)

where we have introduced the dimensionless quantity

$$
\delta m = \ln\left(\hat{\xi}_b/\hat{\gamma}_d\right)
$$

(35)

as a measure of the difference in magnitude between the qubit and the field barrier $f_1$.

In Figure 6 that follows, we depict the variation of the ratio $T_{Hd}^{f_1}/T_{Hd/WKB}$ with quantity $\delta m$. It is clearly seen that as $\delta m$ increases, the normalised Hadamard Time tends to unity, since then the field barrier becomes almost impenetrable and the Hadamard Time coincides with the one from the WKB approximation. On the contrary when the difference in magnitude between the qubit and the field barrier becomes negligible, Hadamard Time increases a lot.
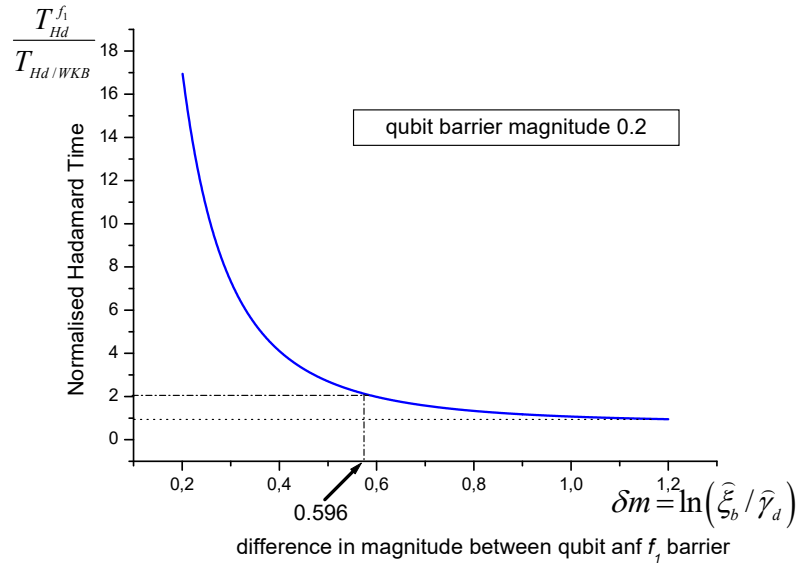
**FIGURE 6.** The normalised Hadamard Time as a function of the difference in magnitude between the field and the qubit barrier. Hadamard Time tends to the WKB expression as the difference in magnitude increases and reaches a value twice the WKB one, for a difference in magnitude of the two barriers equal to 0.596.

iii) Both field barriers $f_1$ and $f_2$ active.

According to (B-12) the real parts of the energy splitting, read

$$
E_o^{L,\bar{\times},R,\bar{\times},\bar{\times}} = E_o - \frac{\left\{ \begin{array}{l} \left(\mp 2\hat{\xi}_{b,o} - \dfrac{\hat{\delta}_{a,o}{}^2}{4}\right)\left\{\left\{d^{E_o}\bar{\vartheta}(b)\right\}\left(4 + \hat{\xi}_{b,o}{}^2 - \dfrac{\hat{\delta}_{a,o}{}^2}{4}\right) - \dfrac{\hat{\delta}_{a,o}{}^2}{2}\left\{d^{E_o}\hat{\delta}(a)\right\} \pm 2\hat{\xi}_{b,o}\left\{d^{E_o}\hat{\xi}(b)\right\}\right\} \\ + \left(-2\hat{\xi}_{b,o}{}^2 - \dfrac{\hat{\delta}_{a,o}{}^2}{4}\right)\left\{2\hat{\xi}_{b,o}{}^2\left(\left\{d^{E_o}\hat{\xi}(b)\right\} \mp \hat{\xi}_{b,o}{}^{-1}\left\{d^{E_o}\bar{\vartheta}(b)\right\} \pm 2\left\{d^{E_o}\bar{\vartheta}(b)\right\}\dfrac{\hat{\xi}_{b,o}{}^{-1}\hat{\gamma}_{d,o}{}^2}{\hat{\gamma}_{d,o}{}^2 - \hat{\xi}_{b,o}{}^2}\right) - \dfrac{\hat{\delta}_{a,o}{}^2}{2}\left(\dfrac{1}{2}\left\{d^{E_o}\bar{\vartheta}(b)\right\} + \left\{d^{E_o}\hat{\delta}(a)\right\}\right)\right\} \end{array}\right\}}{\left\{ \begin{array}{l} \left\{\left\{d^{E_o}\bar{\vartheta}(b)\right\}\left(-4 + \hat{\xi}_{b,o}{}^2 - \dfrac{\hat{\delta}_{a,o}{}^2}{4}\right) \pm 2\hat{\xi}_{b,o}\left\{d^{E_o}\hat{\xi}(b)\right\} - \dfrac{\hat{\delta}_{a,o}{}^2}{2}\left\{d^{E_o}\hat{\delta}(a)\right\}\right\}^2 + \\ \left\{2\hat{\xi}_{b,o}{}^2\left(\left\{d^{E_o}\hat{\xi}(b)\right\} \mp \hat{\xi}_{b,o}{}^{-1}\left\{d^{E_o}\bar{\vartheta}(b)\right\} \pm 2\left\{d^{E_o}\bar{\vartheta}(b)\right\}\dfrac{\hat{\xi}_{b,o}{}^{-1}\hat{\gamma}_{d,o}{}^2}{\hat{\gamma}_{d,o}{}^2 - \hat{\xi}_{b,o}{}^2}\right) - \dfrac{\hat{\delta}_{a,o}{}^2}{2}\left(\dfrac{1}{2}\left\{d^{E_o}\bar{\vartheta}(b)\right\} + \left\{d^{E_o}\hat{\delta}(a)\right\}\right)\right\}^2 \end{array}\right\}}
$$

(36)

Thus, we get for the Hadamard Time the following expression:

$$
\frac{T_{Hd}^{f_1,f_2}}{T_{Hd/WKB}} = \frac{T_{Hd}^1 T_{Hd}^2}{T_{Hd/WKB}\left(T_{Hd}^1 - T_{Hd}^2\right)}
$$

(37)

with

$$T_{Hd}^{2(top\ sign)}_{\phantom{Hd}1(down\ sign)} = T_{Hd/WKB} \dfrac{\left(-4\pm 2\,sim(\widehat{\breve{\xi}},\breve{\vartheta})\widehat{\xi}_{b,o}-sim(\widehat{\delta},\breve{\vartheta})\dfrac{\widehat{\delta}_{a,o}^2}{2}\right)^2+\left(\mp 2\widehat{\breve{\xi}}\left(1-2\dfrac{e^{2\delta m}}{e^{2\delta m}-1}\right)\right)^2}{\left[\begin{array}{l}\left\{\left[\left(-4\widehat{\xi}_{b,o}-\dfrac{\widehat{\delta}_{a,o}^2}{2}\right)\left(\mp 2\pm 4\dfrac{e^{2\delta m}}{e^{2\delta m}-1}\right)-\dfrac{5}{4}\widehat{\xi}_{b,o}^{-1}\widehat{\delta}_{a,o}^2\mp 8\right\}+\right.\\ \left\{sim(\widehat{\breve{\xi}},\breve{\vartheta})\left(-4\widehat{\xi}_{b,o}+2\widehat{\xi}_{b,o}\left(-2\widehat{\xi}_{b,o}^2-\dfrac{\widehat{\delta}_{a,o}^2}{4}\right)\right)\right\}+\\ \left\{sim(\widehat{\delta},\breve{\vartheta})\left(\pm\widehat{\delta}_{a,o}^2+\dfrac{\widehat{\delta}_{a,o}^2}{2}\left(2\widehat{\xi}_{b,o}-\dfrac{\widehat{\xi}_{b,o}^{-1}\widehat{\delta}_{a,o}^2}{4}\right)\right)\right\}\end{array}\right]} \tag{38}$$

In Table 3 that follows we include the values of various parameters that were employed in (38), as these were taken from our previous results.

| Parameter | Value |
|---|---|
| Qubit barrier strength $\varphi(\lambda)$ (Figure 5) | 0.20 / 0.35 |
| Difference in strength $\delta m = \ln\left(\widehat{\xi}_b / \widehat{\gamma}_d\right)$ for 200% of the WKB value of the Hadamard Time (Figure 6) | 0.596 / 0.693 |
| $sim(\widehat{\breve{\xi}},\breve{\vartheta})$: similarity factor for minimum value of the normalized Hadamard Time in (Figure 5) | 1.39 / 1.69 |
| $\delta$ field barrier magnitude | 0.35 |

**TABLE 3.** The values of the parameters used in (38) for producing Figure 7

Thus we produce Figure 7 that follows, where **t**he variation of the normalised Hadamard Time as a function of the similarity factor $sim(\widehat{\delta},\breve{\vartheta})$ is depicted.
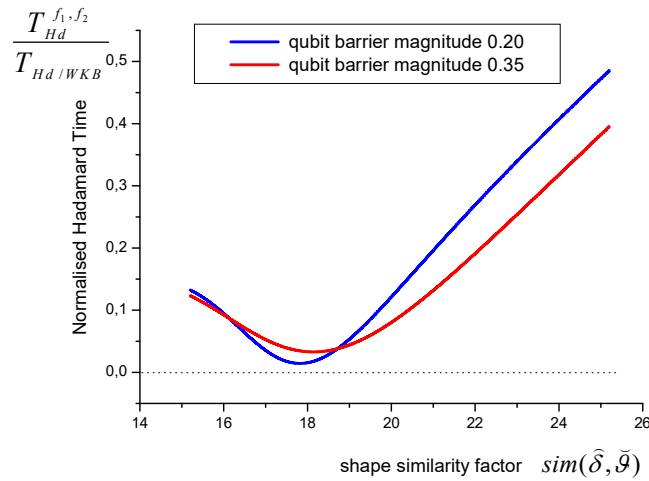
**FIGURE 7.** The variation of the normalised Hadamard Time as a function of the similarity factor $sim(\widehat{\delta}, \breve{\vartheta})$ which relates the change of the $\delta$ field barrier magnitude to the change of the well magnitude with energy increament, for two different values of the qubit barrier magnitude.

As far as the imaginary part is concerned, we should point out that this contributes to the exponential decay rate of the initial state. This can be seen by taking the Fourier transform of the Breit-Wigner or Lorentzian decay amplitude

$$Gr(E) = \frac{i}{E - \left( E_o + \delta E_O - i\frac{\Gamma_o}{2} \right)} \tag{39}$$

and extending the spectrum to the full real axis $-\infty < E < \infty$ instead of being bounded from below $0 \le E < \infty$ ("Fermi's approximation"). The time evolution of the decaying state is then given by

$$\Psi(t) = e^{-i(E_o + \delta E_o)t/\hbar} e^{-\Gamma_o t/2\hbar} \Psi(0) \tag{40}$$

Thus the survival probability of the initial state is given as

$$P(t) \sim {}^{-\Gamma_o t/\hbar} \tag{41}$$

and this is called exponential decay. The decoherence of a quantum superposition state due to its interaction with the environment leads to an exponential decay law, [65,66]. Thus, $\hbar/\Gamma o$ is a meter of the qubit's decoherence time, meaning the time interval that the coherent superposition state survives. However if we do not necessarily extend the spectrum we will also find non exponential contributions for both small and large times. As far as the region of large times is concerned the non exponential contribution dominates the system's evolution and takes the following form, [64],

$$P(t) \sim \left\{ \left\{ \left( E_o + \delta E_O \right)^2 + \frac{\Gamma_o{}^2}{4} \right\} t^2 \right\}^{-1} \tag{42}$$

In Figure 8 that follows we depict exponential decay rates $\Gamma_o^{L,\breve{\times},R,\breve{\times}}$ and $\Gamma_o^{L,\breve{\times},R,\breve{\times},\breve{\times}}$ which are twice the imaginary parts of (B-9) and (B-12) respectively, as a function of the similarity factor $sim(\hat{\xi},\breve{\vartheta})$, for the parameter values contained in Table 5. In addition we extract the value of 18.2 for the similarity factor $sim(\hat{\delta},\breve{\vartheta})$, taken from Figure 7, which makes the corresponding Hadamard Time a minimum.

.
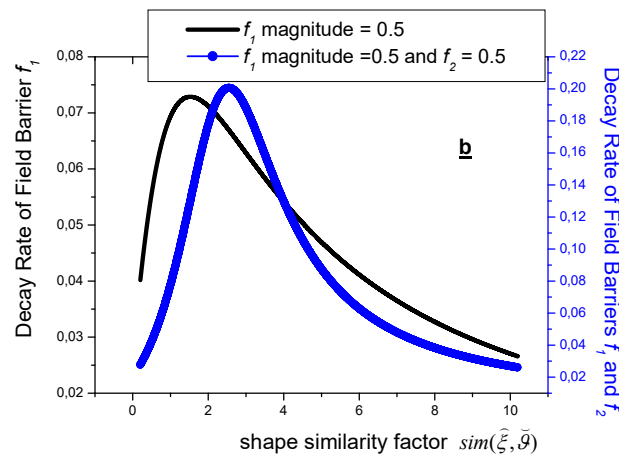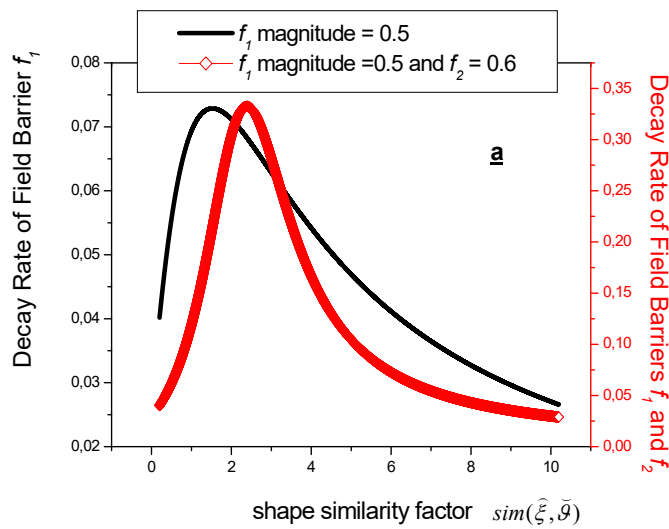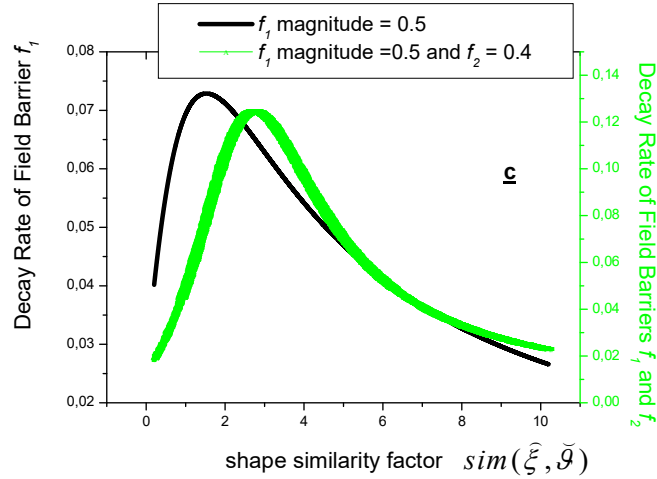
**FIGURE 8.** Comparison of the exponential decay rate for barrier field $f_1$ only active and both barrier fields $f_1$ and $f_2$ active, as a function of the similarity factor $sim(\widehat{\xi}, \breve{\vartheta})$, for three different cases as far as the relative magnitude of the field barriers is concerned: a) $f_1 < f_2$ b) $f_1 = f_2$, c) $f_1 > f_2$. Note that the two rates come in different orders of magnitude.

# CONCLUDING REMARKS

In this paper, we studied the dynamics of a positional-based qubit structure as this is induced and controlled by the presence of two independent electrostatic fields. Our attention focused on the Hadamard Time, defined in the present paper as the time needed for the initial state to come in an equally weighted coherent superposition of the two orthogonal qubit states $|0\rangle$ and $|1\rangle$, through the particle's probabilistic appearance in both quantum wells. First, we analytically solved the model providing analytical relations for the system's Green function and energy eigenvalues. Second, we gave analytical expressions for the intrinsic qubit's time needed for oscillation between its orthogonal states and more than this of the time required for decoherence to appear through exponential decay.

In quantum computation, knowledge of the Hadamard Time is significant since it corresponds to the knowledge of the time needed for quantum coherent superposition to appear. The latter makes a substantial difference to quantum computing compared to its classical counterpart and makes quantum calculations much faster and the quantum computational system itself much more capable, [1]. Thus, in order to carry out quantum computations we should, at first, adjust the clock frequency of the computational system to the "frequency" $f = 1/T_{Hd}$ of series of revivals of the superposition state. One can produce entangled states through such suitably prepared superposition states, [67]. Thus, frequency adjustment is required for quantum cryptography as well. In addition, our computing system gets less complicated since now no Hadamard gate is needed. At the same time, decoherence is unavoidable due to the qubit's interaction with the environment. Decoherence destroys quantum superposition and forces the system to decay. The exponential decay rates that we analytically calculated in the current paper provide a decoherence time scale for the

duration of the computational calculations, maintaining their effectivity and accuracy. Decoherence time should be much longer than the period of revivals of the superposition state, [48]. In addition, the analytic study of the above phenomena through path integral theory provides more insight into the physics of the system.

In particular equation (30) gives the Hadamard Time in the case of the unperturbed or ideally isolated qubit. Clearly our result goes far beyond the WKB expression. But most importantly introduces quantity $sim(\hat{\bar{\xi}}, \breve{\vartheta})$, defined as the similarity factor that relates the shape of the well to the one of the barrier as explained in Figure 4. As far as our knowledge goes this quantity has never before been introduced in the international bibliography. It is some kind of correction to the phase event reflection factors that contribute to the path integral calculation, (see the discussion at the end of the first section). In Figure 5 that follows eq. (30), we have depicted the dependence of the normalized (to the WKB expression) Hadamard Time on the similarity factor $sim(\hat{\bar{\xi}}, \breve{\vartheta})$, for two different values of the qubit barrier magnitude. The Hadamard Time receives a minimum value. Both the minimum and the minimum position are increasing functions of the qubit barrier magnitude. Thus the DWP can be suitably engineered for Hadamard Time to receive its minimum value. The latter is very important since then small variations in the qubit's potential will not alter Hadamard Time and consequently will not change the time scale of computation ensuring stability. Hadamard Time tends to a constant value when the well and the barrier are not shape related, $sim(\hat{\bar{\xi}}, \breve{\vartheta}) = 0$, but increases unlimited as $sim(\hat{\bar{\xi}}, \breve{\vartheta})$ increases, since then the qubit barrier becomes almost impenetrable.

For the case of the field barrier $f_1$ alone, which permits the interaction of the qubit state with the continuum, eq. (33) describes the dependence of the Hadamard Time on the difference in magnitude of the qubit and the field barrier, with the later expressed through quantity $\delta m$ defined in (34). In Figure 6 we depict the above mentioned dependence for a qubit barrier magnitude equal to 0.2. It is clearly seen that the Hadamard Time tends to the WKB expression as the difference in magnitude increases, since then the field barrier becomes impenetrable. On the other hand as the magnitude of the field barrier is lowered approaching the one of the qubit barrier, Hadamard Time increases, since then tunnelling is equally preferable by both mechanisms: internal oscillation and external diffusion to the continuum. Giving an example, Hadamard Time becomes twice the WKB expression for a difference in barrier magnitude nearly equal to 0.6. The field barrier magnitude is directly dependent on the field strength imposed on the qubit. Hence a suitably engineered DWP and a suitable applied electrostatic field $f_1$, including its starting point and slope, uniquely determine the computational time scale.

When both field barriers are active, we are interested not only for the change in Hadamard Time but for the change of the exponential decay rate as well, compared to the case of the field $f_1$ alone. Thus, in Figure 7 we depict the dependence of the Hadamard Time with the factor $sim(\hat{\delta}, \breve{\vartheta})$ which relates the change of the $\delta$ field barrier magnitude to the change of the well magnitude with energy increament, for two different values of the qubit barrier magnitude. The Hadamard Time becomes minimum for a certain value of the similarity function. Both the minimum value and the minimum position are increasing functions of the qubit barrier magnitude. Quite impressively, the minimum region corresponds to much larger values of the similarity factor compared to the case of the perfectly isolated DWP. Actually, their difference is equal to one order of magnitude. In addition, minimum Hadamard Time becomes much smaller, enabling fast but still stable quantum calculations. Interestingly

enough, the curve corresponding to the larger qubit barrier, is positioned under the smaller qubit barrier curve, after a characteristic value of the similarity factor.

As far as the exponential decay rate is concerned, we compare the case where both field barriers, $f_1$ and $f_2$, are present, with the one where only the field barrier $f_1$ is active. In Figure 8, we have sketched the decay rate as a function of the similarity factor $sim(\breve{\xi}, \breve{\mathcal{G}})$, for the previously mentioned field presences, examining separately three different values of the $f_2$ magnitude: greater, equal and less than the $f_1$ magnitude where the latter is assumed to remain constant. In each case the two rates come in different orders of magnitude and their difference is an increasing function of the $f_2$ barrier magnitude. Hence, the qubit state decays much faster due to the presence of a double field barrier. However, for large values of the similarity factor, the two rates become nearly equal, since then the dominant mechanism is the internal oscillation and not decoherence. Finally, let us assume that $f_1$ stands for the system intera-ction with its environment while $f_2$ electrostatically controls the qubit. Interestingly enough, the case of nearly equal barriers, as is shown in figure 8c, does not speed up the system's decay compared to the situation where control is absent. In other words, we can control the qubit without accelerating its decoherence.

# APPENDIX A:
## Analytic calculation of the propagation amplitudes beyond $Y^L$.

i)  Transition Amplitude $\Upsilon^{L,\breve{\times}}$

This includes propagation inside the classically allowed region of state $|0\rangle$ and the classically forbidden internal barrier $\overleftrightarrow{\times}$. This will affect the eigenvalues of state $|0\rangle$ which will be naturally perturbed. We use the following symbolism: $\Upsilon^{L,\breve{\times}} \equiv \left\{ L \rightleftarrows_{r_1}^{b} \breve{\times} \right\} A_L(b; r_2)$, in order to indicate the fact that we must first alternate region L with the one of the internal barrier, in all possible (infinite) ways between points $r_1$ and b, and then propagate in all possible ways from point $b$ to $r_2$, while staying at region L. So, we must first come to point $b$ which is common for the two regions and this results to $A_L(r_1; b)$. Then we interchange the two regions in all possible ways, starting and ending at turning point $b$. We finally propagate inside region L, between $b$ and $r_2$. According to the above we have:

$$\Upsilon^{L,\breve{\times}} = A_L(r_1; b) A_{\breve{\times}}(b; b) \left\{ 1 - A_L(b; b) A_{\breve{\times}}(b; b) \right\}^{-1} A_L(b; r_2) \tag{A-1}$$

Repeating the procedure of the previous paragraph, by substituting the phase event factors and doing the tedious algebra we find:

$$\Upsilon^{L,\breve{\times}} = -2 \frac{\operatorname{Im} \breve{\mathcal{G}}_{r_1}^{\pi/4} \operatorname{Im} \breve{\mathcal{G}}_{r_2}^{\pi/4}}{\breve{\mathcal{G}}_b} \left\{ \frac{1}{\operatorname{Re} \breve{\mathcal{G}}_b} - \frac{1}{\operatorname{Re} \breve{\mathcal{G}}_b - \dfrac{\breve{\mathcal{G}}_b \breve{\xi}_b^2}{4 + \breve{\xi}_b^2}} \right\} \tag{A-2}$$

ii)       Transition Amplitude $\Upsilon^{L,\breve{x},R}$

In this case state $|0\rangle$ not only interacts with the internal barrier but with state $|1\rangle$ as well. It is obvious that we must first come to turning point $c$, by interchanging in all possible ways the regions of L, $\breve{x}$, R , and then interchange the couples (L,$\breve{x}$ ) and (R, $\breve{x}$ ) in all possible ways. Finally we can propagate to point $r_2$ through the couple (L,$\breve{x}$ ) or by staying entirely at region L. Putting all these together we get

$$\Upsilon^{L,\breve{x},R} = \left\{L \underset{r_1}{\overset{c}{\rightleftarrows}} \breve{x}\right\}\left\{|q\rangle \underset{c}{\overset{b}{\rightleftarrows}} \breve{x}\right\}\left[1-\left\{L \underset{b}{\overset{c}{\rightleftarrows}} \breve{x}\right\}\left\{R \underset{c}{\overset{b}{\rightleftarrows}} \breve{x}\right\}\right]^{-1}\left[\left\{L \underset{b}{\overset{r_2}{\rightleftarrows}} \breve{x}\right\} + A_L(b;r_2)\right]$$

(A-3)

Table $A_1$ that follows contains the above coupled regions propagation amplitudes as these are calculated in terms of fundamental amplitudes:

| Amplitudes for the regions  L, $\breve{x}$ , R | Function of Fundamental Amplitudes |
|---|---|
| $\left\{L \underset{r_1}{\overset{c}{\rightleftarrows}} \breve{x}\right\}$ | $A_L(r_1;b)A_{\breve{x}}(b;c)\left\{1 - A_L(b;b)A_{\breve{x}}(b;b)\right\}^{-1}$ |
| $\left\{L \underset{b}{\overset{c}{\rightleftarrows}} \breve{x}\right\}$ | $A_L(b;b)A_{\breve{x}}(b;c)\left\{1 - A_L(b;b)A_{\breve{x}}(b;b)\right\}^{-1}$ |
| $\left\{L \underset{b}{\overset{r_2}{\rightleftarrows}} \breve{x}\right\}$ | $A_L(b;b)A_{\breve{x}}(b;b)\left[1 - A_L(b;b)A_{\breve{x}}(b;b)\right]^{-1} A_L(b;r_2)$ |
| $\left\{R \underset{c}{\overset{b}{\rightleftarrows}} \breve{x}\right\}$ | $A_R(c;c)A_{\breve{x}}(c;b)\left\{1 - A_R(c;c)A_{\breve{x}}(c;c)\right\}^{-1}$ |

**TABLE A₁.** Calculation of the coupled regions ({L, $\breve{x}$ }, {R, $\breve{x}$ }) path integral amplitudes in terms of fundamental amplitudes.

Repeating the procedure of the previous paragraph, by substituting the phase event factors and completing the tedious algebra, we find:

$$\Upsilon^{L,\breve{x},R} = 2\frac{\operatorname{Im}\breve{\vartheta}_{r_1}^{\pi/4}\operatorname{Im}\breve{\vartheta}_{r_2}^{\pi/4}}{\breve{\vartheta}_b}\left\{2\left\{\begin{array}{l}\operatorname{Re}\breve{\vartheta}_b - \dfrac{\breve{\xi}_b^2\left(\pm 2\operatorname{Im}\breve{\vartheta}_b\breve{\xi}_b^{-1} + \operatorname{Re}\breve{\vartheta}_b\right)}{4+\breve{\xi}_b^2} + \\[2mm] i\,\dfrac{\breve{\xi}_b^2\left(\pm 2\operatorname{Re}\breve{\vartheta}_b\breve{\xi}_b^{-1} - \operatorname{Im}\breve{\vartheta}_b\right)}{4+\breve{\xi}_b^2}\end{array}\right\}^{-1} - \dfrac{1}{\operatorname{Re}\breve{\vartheta}_b - \dfrac{\breve{\vartheta}_b\breve{\xi}_b^2}{4+\breve{\xi}_b^2}}\right\}$$

(A-4)

where the twofold symbols $\pm$ that appear in the first fractional term, mean that we must actually sum two fractions, one for each sign.

iii)    Transition Amplitude $\Upsilon^{L,\vec{\times},R,\vec{\times}}$

In this case state $|0\rangle$ not only interacts with state $|1\rangle$ through the internal barrier but with the field barrier $\vec{\times}$ as well. This will force the system to decay. It is obvious that we must first combine the three regions L, $\vec{\times}$, R, by propagating from $r_1$ to turning point $d$, and then combine regions $\vec{\times}$,R,$\vec{\times}$, by propagating from $d$ to $b$, and then alternate the couple (L,$\vec{\times}$) with (R,$\vec{\times}$) in all possible ways. Finally we can propagate to point $r_2$ through the couple (L,$\vec{\times}$) or by staying entirely at region L. Putting all these together we get:

$$\Upsilon^{L,\vec{\times},R,\vec{\times}} = \left\{ L \underset{r_1}{\overset{c}{\rightleftarrows}} \vec{\times} \right\} A_R(c;d) \left[ 1 + \left\{ R \underset{c}{\overset{c}{\rightleftarrows}} \vec{\times} \right\} \right] \left[ 1 - \left\{ R \underset{c}{\overset{b}{\rightleftarrows}} \vec{\times} \right\} \left\{ L \underset{b}{\overset{c}{\rightleftarrows}} \vec{\times} \right\} \right]^{-1}$$

$$\left\{ \vec{\times} \underset{d}{\overset{c}{\rightleftarrows}} R \right\} A_{\vec{\times}}(c;b) \left[ 1 + \left\{ \vec{\times} \underset{c}{\overset{c}{\rightleftarrows}} R \right\} \right] \left[ 1 - \left\{ \vec{\times} \underset{c}{\overset{d}{\rightleftarrows}} R \right\} \left\{ \vec{\times} \underset{d}{\overset{c}{\rightleftarrows}} R \right\} \right]^{-1}$$

$$\left[ 1 - (-i) A_L(r_1;b) \left\{ L \underset{r_1}{\overset{c}{\rightleftarrows}} \vec{\times} \right\} A_R(c;d) \left[ 1 + \left\{ R \underset{c}{\overset{c}{\rightleftarrows}} \vec{\times} \right\} \right] \left[ 1 - \left\{ R \underset{c}{\overset{b}{\rightleftarrows}} \vec{\times} \right\} \left\{ L \underset{b}{\overset{c}{\rightleftarrows}} \vec{\times} \right\} \right]^{-1} \right.$$ 

$$\left. \left\{ \vec{\times} \underset{d}{\overset{c}{\rightleftarrows}} R \right\} A_{\vec{\times}}(c;b) \left[ 1 + \left\{ \vec{\times} \underset{c}{\overset{c}{\rightleftarrows}} R \right\} \right] \left[ 1 - \left\{ \vec{\times} \underset{c}{\overset{d}{\rightleftarrows}} R \right\} \left\{ \vec{\times} \underset{d}{\overset{c}{\rightleftarrows}} R \right\} \right]^{-1} \right]^{-1} \quad \text{(A-5)}$$

$$\left[ 1 + \left\{ L \underset{b}{\overset{c}{\rightleftarrows}} \vec{\times} \right\} \left\{ R \underset{c}{\overset{c}{\rightleftarrows}} \vec{\times} \right\} \left[ 1 - \left\{ R \underset{c}{\overset{b}{\rightleftarrows}} \vec{\times} \right\} \left\{ L \underset{b}{\overset{c}{\rightleftarrows}} \vec{\times} \right\} \right]^{-1} \right] \left[ 1 + \left\{ L \underset{b}{\overset{b}{\rightleftarrows}} \vec{\times} \right\} \right] A_L(b;r_2)$$

In Table $A_2$ that follows we have calculated the coupled regions propagation amplitudes of this category, in terms of fundamental amplitudes.

| Amplitudes of the regions L,$\vec{\times}$ , R | Function of Fundamental Amplitudes |
|---|---|
| $\left\{ R \underset{c}{\overset{c}{\rightleftarrows}} \vec{\times} \right\}$ | $A_R(c;c) A_{\vec{\times}}(c;c) \left[ 1 - A_R(c;c) A_{\vec{\times}}(c;c) \right]^{-1}$ |
| $\left\{ L \underset{b}{\overset{b}{\rightleftarrows}} \vec{\times} \right\}$ | $A_L(b;b) A_{\vec{\times}}(b;b) \left[ 1 - A_L(b;b) A_{\vec{\times}}(b;b) \right]^{-1}$ |
| $\left\{ \vec{\times} \underset{c}{\overset{d}{\rightleftarrows}} R \right\}$ | $A_R(c;d) A_{\vec{\times}}(c;c) \left[ 1 - A_R(c;c) A_{\vec{\times}}(c;c) \right]^{-1}$ |
| $\left\{ \vec{\times} \underset{c}{\overset{c}{\rightleftarrows}} R \right\}$ | $A_R(c;c) A_{\vec{\times}}(c;c) \left[ 1 - A_R(c;c) A_{\vec{\times}}(c;c) \right]^{-1}$ |
| $\left\{ \vec{\times} \underset{d}{\overset{c}{\rightleftarrows}} R \right\}$ | $A_{\vec{\times}}(d;d) A_R(c;d) \left[ 1 - A_{\vec{\times}}(d;d) A_R(c;c) \right]^{-1}$ |

**TABLE $A_2$.** Calculation of the coupled regions ({R, $\vec{\times}$ }, {L, $\vec{\times}$ }, { $\vec{\times}$ ,L}) path integral amplitudes in terms of fundamental amplitudes.

The field barrier $\vec{\times}$ acquires a phase factor and forms the following barrier magnitude $\exp\left[-\left|\int_d^e \tau(y)dy\right|\right] \equiv e^{-\gamma(d)} \equiv \hat{\gamma}_d$. Putting the above together and completing the tedious algebra, we finally get:

$$\Upsilon^{L,\vec{\times},R,\vec{\times}} = 2\frac{\operatorname{Im}\breve{\vartheta}_{r_1}^{\pi/4}\operatorname{Im}\breve{\vartheta}_{r_2}^{\pi/4}}{\breve{\vartheta}_b}\left\{ -\frac{1}{2\left\{\operatorname{Re}\breve{\vartheta}_b - \frac{\breve{\xi}_b^{\ 2}\left[\left(\pm 2\operatorname{Im}\breve{\vartheta}_b\breve{\xi}_b^{-1} + \operatorname{Re}\breve{\vartheta}_b\right)+ \atop i\left(\pm 2\operatorname{Re}\breve{\vartheta}_b\breve{\xi}_b^{-1} - \operatorname{Im}\breve{\vartheta}_b\right)\right]}{4+\breve{\xi}_b^{\ 2}}\right\}} + \frac{1}{4\operatorname{Re}\breve{\vartheta}_b - \breve{\xi}_b^{\ 2}\breve{\vartheta}_b \pm \frac{\rho}{\breve{\vartheta}_b}}\right\} \qquad (A\text{-}6)$$

where quantity $\rho$ is defined as

$$\rho = \left\{-4\breve{\xi}_b^{\ 2}\breve{\vartheta}_b^{\ 4} + \frac{\left(4\breve{\xi}_b\hat{\gamma}_d\right)^2\breve{\vartheta}_b^{\ 3}\operatorname{Re}\breve{\vartheta}_b}{\left(4\operatorname{Re}\breve{\vartheta}_b - \breve{\xi}_b^{\ 2}\breve{\vartheta}_b\right)^2 + \left(\breve{\xi}_b\hat{\gamma}_d\right)^2}\right\}^{1/2} \qquad (A\text{-}7)$$

Again the symbol $\pm$ that appears in eq. (18), means that we must actually sum two fractions, one for each sign.

iv)     Transition Amplitude $\Upsilon^{L,\vec{\times},R,\vec{\times},\vec{\times}}$

State $|1\rangle$ has already interacted with the total region on its right side, before reaching point $a$ in order to interact with the second field barrier $\vec{\times}$. A second channel of decay appears now. Thus we need to modify all the previously calculated transition amplitudes in such a way that propagation ends at turning point $a$ instead of $r_2$. Thus we use the symbol $\Upsilon^{L+\vec{\times}+R+\vec{\times}}(r_1; a)$ to describe the sum of the previously calculated amplitudes for $r_2 = a$. Modifying in this way the amplitudes we get:

$$\Upsilon^L_{r_1 \to a} = \vec{A}_L(r_1; a) + \vec{A}_L(r_1; a)(-i)A_L(a; a) + \vec{A}_L(r_1; b)(-i)A_L(b; a) \qquad (A\text{-}8)$$

$$\Upsilon^{L,\vec{\times}}_{r_1 \to a} = A_L(r_1; b)A_{\vec{\times}}(b; b)\left\{1 - A_L(b; b)A_{\vec{\times}}(b; b)\right\}^{-1}A_L(b; a) \qquad (A\text{-}9)$$

$$\Upsilon^{L,\vec{\times},R}_{r_1 \to a} = \left\{L \rightleftarrows_{r_1}^c \vec{\times}\right\}\left\{R \rightleftarrows_c^b \vec{\times}\right\}\left[1 - \left\{L \rightleftarrows_b^c \vec{\times}\right\}\left\{R \rightleftarrows_c^b \vec{\times}\right\}\right]^{-1}\left[\left\{L \rightleftarrows_b^{r_2} \vec{\times}\right\}A_L(b; a)\right] \qquad (A\text{-}10)$$

$$\Upsilon_{r_1 \to a}^{L,\bar{\times},R,\bar{\times}} = \left\{ L \underset{r_1}{\overset{c}{\rightleftarrows}} \triangle \right\} A_R(c;d) \left[ 1 + \left\{ R \underset{c}{\overset{c}{\rightleftarrows}} \bar{\times} \right\} \right] \left[ 1 - \left\{ R \underset{c}{\overset{b}{\rightleftarrows}} \bar{\times} \right\} \left\{ R \underset{b}{\overset{c}{\rightleftarrows}} \bar{\times} \right\} \right]^{-1}$$

$$\left\{ \bar{\times} \underset{d}{\overset{c}{\rightleftarrows}} R \right\} A_{\bar{\times}}(c;b) \left[ 1 + \left\{ \bar{\times} \underset{c}{\overset{c}{\rightleftarrows}} R \right\} \right] \left[ 1 - \left\{ \bar{\times} \underset{c}{\overset{d}{\rightleftarrows}} R \right\} \left\{ \bar{\times} \underset{d}{\overset{c}{\rightleftarrows}} R \right\} \right]^{-1}$$

$$\left[ 1 - (-i) A_L(r_1;b) \left\{ L \underset{r_1}{\overset{c}{\rightleftarrows}} \bar{\times} \right\} A_R(c;d) \left[ 1 + \left\{ R \underset{c}{\overset{c}{\rightleftarrows}} \bar{\times} \right\} \right] \left[ 1 - \left\{ R \underset{c}{\overset{b}{\rightleftarrows}} \bar{\times} \right\} \left\{ L \underset{b}{\overset{c}{\rightleftarrows}} \bar{\times} \right\} \right]^{-1} \right]^{-1}$$

$$\left. \left\{ \bar{\times} \underset{v}{\overset{\mu}{\rightleftarrows}} R \right\} A_{\bar{\times}}(c;b) \left[ 1 + \left\{ \bar{\times} \underset{c}{\overset{c}{\rightleftarrows}} R \right\} \right] \left[ 1 - \left\{ \bar{\times} \underset{c}{\overset{d}{\rightleftarrows}} R \right\} \left\{ \bar{\times} \underset{d}{\overset{c}{\rightleftarrows}} R \right\} \right]^{-1} \right]$$

$$\left[ 1 + \left\{ L \underset{b}{\overset{c}{\rightleftarrows}} \bar{\times} \right\} \left\{ R \underset{c}{\overset{c}{\rightleftarrows}} \bar{\times} \right\} \left[ 1 - \left\{ R \underset{c}{\overset{b}{\rightleftarrows}} \bar{\times} \right\} \left\{ L \underset{b}{\overset{c}{\rightleftarrows}} \bar{\times} \right\} \right]^{-1} \right] \left[ 1 + \left\{ L \underset{b}{\overset{b}{\rightleftarrows}} \bar{\times} \right\} \right] A_L(b;a)$$

<div align="right">(A-11)</div>

Obviously

$$\Upsilon^{L+\bar{\times}+R+\bar{\times}}(r_1;a) = \Upsilon_{r_1 \to a}^{L} + \Upsilon_{r_1 \to a}^{L,\bar{\times}} + \Upsilon_{r_1 \to a}^{L,\bar{\times},R} + \Upsilon_{r_1 \to a}^{L,\bar{\times},R,\bar{\times}} \tag{A-12}$$

The combination of the above with the field barrier $\bar{\times}$, according to our aforementioned directions, gives the following:

$$\Upsilon^{L,\bar{\times},R,\bar{\times},\bar{\times}} = \left[ Y^{L+\bar{\times}+R+\bar{\times}}(r_1;a) A_{\bar{\times}}(a;a) + \left( Y^{L+\bar{\times}+R+\bar{\times}}(r_1;a) A_{\bar{\times}}(a;a) \right)^2 + ... \right] A_L(a;a) =$$

$$Y^{L+\bar{\times}+R+\bar{\times}}(r_1;a) A_{\bar{\times}}(a;a) \left[ 1 - Y^{L+\bar{\times}+R+\bar{\times}}(r_1;a) A_{\bar{\times}}(a;a) \right]^{-1} A_L(a;a) \tag{A-13}$$

where a single propagation inside field barrier $\bar{\times}$ acquires a phase factor that forms the following barrier magnitude $\exp \left[ - \left| \int_0^a \tau(y) dy \right| \right] \equiv e^{-\delta(a)} \equiv \hat{\delta}_a$ and where of course

$$A_{\bar{\times}}(a;a) = \frac{i}{2} \frac{\hat{\delta}_a^2}{1 + \hat{\delta}_a^2 / 4}$$

Putting all these together we get the total transition amplitude for propagation between points $r_1$ and $a$ in the following form

$$\Upsilon^{total} = \Upsilon^{L+\bar{\times}+R+\bar{\times}}(r_1;a) + \Upsilon^{L,\bar{\times},R,\bar{\times},\bar{\times}} \Rightarrow$$

$$\Upsilon^{total} = \Upsilon^{L+\bar{\times}+R+\bar{\times}}(r_1;a) + \frac{\Upsilon^{L+\bar{\times}+R+\bar{\times}}(r_1;a) A_{\bar{\times}}(\alpha;\alpha) A_L(\alpha;\alpha)}{1 - \Upsilon^{|0\rangle+\bar{\times}+|1\rangle+\bar{\times}}(r_1;a) A_{\bar{\times}}(a;a)} \Rightarrow \tag{A-14}$$

$$\Upsilon^{total} = \frac{\Upsilon^{L+\bar{\times}+R+\bar{\times}}(r_1;a) A_{\bar{\times}}(\alpha;\alpha) \left\{ \left( \dfrac{1}{2\bar{\vartheta}_b \, \mathrm{Re}\, \bar{\vartheta}_b} \right) - \Upsilon^{L+\bar{\times}+R+\bar{\times}}(r_1;a) \right\} + \Upsilon^{L+\bar{\times}+R+\bar{\times}}(r_1;a)}{1 - \Upsilon^{L+\bar{\times}+R+\bar{\times}}(r_1;a) A_{\bar{\times}}(a;a)}$$

It is interesting to notice that the pole condition: $1 - \Upsilon^{L+\bar{\times}+R+\bar{\times}}(r_1;a) A_{\bar{\times}}(a;a) = 0$, transforms the total amplitude in its much simpler form

$$\Upsilon^{total} = \frac{1}{2\left\{1 - \Upsilon^{L+\breve{\times}+R+\breve{\times}}(r_1;a)A_{\breve{\times}}(a;a)\right\}\breve{\vartheta}_b \operatorname{Re}\breve{\vartheta}_b} \tag{A-15}$$

## APPENDIX B:

## Analytic calculation of the energy poles of each propagation amplitude beyond that of region L.

Regions L and $\breve{\times}$ contribute with the extra pole term:

$$Pole^{L,\breve{\times}} \sim \left\{ \operatorname{Re}\breve{\vartheta}_b - \frac{\widehat{\xi}_b^{\,2}\breve{\vartheta}_b}{4+\widehat{\xi}_b^{\,2}} \right\}^{-1} \tag{B-1}$$

It is obvious however, that the complex denominator of the above fraction cannot be in any way equal to zero. Thus, we expand the denominator around the eigenvalues of the isolated unperturbed well. Doing so we find

$$Pole_n^{\,L,\breve{\times}} \sim \left\{ E - \left\{ E_n - \widehat{\xi}_{b,n}^{\,2}\frac{d\widehat{\xi}(b)}{dE_n}\left(2\sqrt{2}\frac{d\breve{\vartheta}(b)}{dE_n}\right)^{-2} - i\left(\frac{d\breve{\vartheta}(b)}{dE_n}\right)^{-1}\frac{\widehat{\xi}_{b,n}^{\,2}}{4} \right\} \right\}^{-1} \tag{B-2}$$

Thus the perturbed eigenvalues become complex and equal to

$$Z_n^{L,\breve{\times}} = E_n - \widehat{\xi}_{b,n}^{\,2}\left\{d^{E_n}\widehat{\xi}(b)\right\}\left(2\sqrt{2}\left\{d^{E_n}\breve{\vartheta}(b)\right\}\right)^{-2} - i\left(d^{E_n}\breve{\vartheta}(b)\right)^{-1}\frac{\widehat{\xi}_{b,n}^{\,2}}{4} \tag{B-3}$$

where the subscript $n$ denotes calculation on the eigenvalue $E_n$ and where the symbol $d^{E_n}$ denotes derivation with respect to the eigenvalue $E_n$.

i)     Regions L, $\breve{\times}$ and R contribute with two extra pole terms (one for each sign):

$$Pole^{L,\breve{\times},R} \sim \left\{ 2\left\{ \operatorname{Re}\breve{\vartheta}_b - \frac{\widehat{\xi}_b^{\,2}\left(\pm 2\operatorname{Im}\breve{\vartheta}_b\widehat{\xi}_b^{-1} + \operatorname{Re}\breve{\vartheta}_b\right)}{4+\widehat{\xi}_b^{\,2}} + i\frac{\widehat{\xi}_b^{\,2}\left(\pm 2\operatorname{Re}\breve{\vartheta}_b\widehat{\xi}_b^{-1} - \operatorname{Im}\breve{\vartheta}_b\right)}{4+\widehat{\xi}_b^{\,2}} \right\} \right\}^{-1} \tag{B-4}$$

The two fold signs that appear in the above formula translate to the doublet splitting that was previously described. Hence, we develop the denominator of the above fraction around the eigenvalues $E_n$ of the unperturbed well, to get

$$Pole_n^{L,\bar{\times},R} \sim \cfrac{1}{E - E_n + \cfrac{\hat{\xi}_{b,n}\left(\mp 2 - i\hat{\xi}_{b,n}\right)}{\left\{\left\{d^{E_n}\breve{\mathcal{G}}(b)\right\}\left(-4 + \hat{\xi}_{b,n}{}^2\right) \pm 2\left\{d^{E_n}\hat{\xi}(b)\right\}\hat{\xi}_{b,n}{}^2\right\} + i2\hat{\xi}_{b,n}\left\{\left\{d^{E_n}\hat{\xi}(b)\right\}\hat{\xi}_{b,n} \mp \left(d^{E_n}\breve{\mathcal{G}}(b)\right)\right\}}}$$

$$(B\text{-}5)$$

The perturbed eigenvalues become then complex and equal to

$$z_n^{L,\bar{\times},R} = E_n - \cfrac{\left\{\begin{array}{l} \mp \dfrac{\hat{\xi}_{b,n}}{2}\left\{-\left\{d^{E_n}\breve{\mathcal{G}}(b)\right\}\left(1 - \dfrac{\hat{\xi}_{b,n}{}^2}{4}\right) \pm \left\{d^{E_n}\hat{\xi}(b)\right\}\dfrac{\hat{\xi}_{b,n}}{2}\right\} \\ -i\dfrac{\hat{\xi}_{b,n}}{2}\left\{-\left\{d^{E_n}\breve{\mathcal{G}}(b)\right\}\dfrac{\hat{\xi}_{b,n}}{2}\left(1 - \dfrac{\hat{\xi}_{b,n}{}^2}{4}\right) \pm \left\{d^{E_n}\hat{\xi}(b)\right\}\dfrac{\hat{\xi}_{b,n}{}^2}{4} + \left\{d^{E_n}\hat{\xi}(b)\right\}\hat{\xi}_{b,n}{}^2 \mp \left(\left\{d^{E_n}\breve{\mathcal{G}}(b)\right\}\right)\right\} \end{array}\right\}}{\left\{-\left\{d^{E_n}\breve{\mathcal{G}}(b)\right\}\left(1 - \dfrac{\hat{\xi}_{b,n}{}^2}{4}\right) \pm \left\{d^{E_n}\hat{\xi}(b)\right\}\dfrac{\hat{\xi}_{b,n}}{2}\right\}^2 + \dfrac{\hat{\xi}_{b,n}}{2}\left\{\left\{d^{E_n}\hat{\xi}(b)\right\}\hat{\xi}_{b,n} \mp \left(\left\{d^{E_n}\breve{\mathcal{G}}(b)\right\}\right)\right\}^2}$$

$$(B\text{-}6)$$

ii)      Regions $L, \bar{\times}, R, \bar{\times}$ contribute with two extra pole terms (one for each sign), coming through the fraction:

$$Pole^{L,\bar{\times},R,\bar{\times}} \sim \frac{1}{4\,\mathrm{Re}\,\breve{\mathcal{G}}_b - \breve{\xi}_b{}^2\breve{\mathcal{G}}_b \pm \breve{\mathcal{G}}_b{}^{-1}\rho} \Rightarrow$$

$$Pole^{L,\bar{\times},R,\bar{\times}} \sim \cfrac{1}{4\,\mathrm{Re}\,\breve{\mathcal{G}}_b - \breve{\xi}_b{}^2\breve{\mathcal{G}}_b \pm \left\{-4\breve{\xi}_b{}^2\breve{\mathcal{G}}_b{}^2 + \cfrac{\left(4\breve{\xi}_b\hat{\gamma}_d\right)^2 \breve{\mathcal{G}}_b\,\mathrm{Re}\,\breve{\mathcal{G}}_b}{\left(4\,\mathrm{Re}\,\breve{\mathcal{G}}_b - \breve{\xi}_b{}^2\breve{\mathcal{G}}_b\right)^2 + \left(\breve{\xi}_b\hat{\gamma}_d\right)^2}\right\}^{1/2}}$$

$$(B\text{-}7)$$

For once more, we develop the denominator around the eigenvalues $E_n$ of the unperturbed well to get

$$Pole_n^{L,\bar{\times},R,\bar{\times}} \sim \left\{(E - E_n)\left\{\begin{array}{l} \left(-i\hat{\xi}_{b,n} \mp 2\right) + \\ -4\left\{d^{E_n}\breve{\mathcal{G}}(b)\right\} + 2i\hat{\xi}_{b,n}{}^2\left\{d^{E_n}\hat{\xi}(b)\right\} + \left\{d^{E_n}\breve{\mathcal{G}}(b)\right\}\hat{\xi}_{b,n}{}^2 \\ \mp \hat{\xi}_{b,n}\left(-2\left\{d^{E_n}\hat{\xi}(b)\right\} + 2i\left\{d^{E_n}\breve{\mathcal{G}}(b)\right\} - 4i\dfrac{\left\{d^{E_n}\breve{\mathcal{G}}(b)\right\}e^{-2\gamma_n(v)}}{\hat{\gamma}_{d,n}{}^2 - \hat{\xi}_{b,n}{}^2}\right) \end{array}\right\}\right\}^{-1}$$

$$(B\text{-}8)$$

Thus the perturbed eigenvalues become complex and equal to

$$Z_n^{L,\vec{\times},R,\vec{\times}} = E_n - \frac{\left\{\mp 2\widehat{\xi}_{b,n}\left\{\left\{d^{E_n}\breve{\vartheta}(b)\right\}\left(4-\widehat{\xi}_{b,n}^{\ 2}\right)\pm 2\widehat{\xi}_{b,n}^{\ 2}\left\{d^{E_n}\widehat{\xi}(b)\right\}\right\}+2\widehat{\xi}_{b,n}^{\ 4}\left(\left\{d^{E_n}\widehat{\xi}(b)\right\}\mp\widehat{\xi}_{b,n}\left\{d^{E_n}\breve{\vartheta}(b)\right\}-2\frac{\left\{d^{E_n}\breve{\vartheta}(b)\right\}\widehat{\gamma}_{d,n}^{\ 2}}{\left(\widehat{\gamma}_{d,n}\widehat{\xi}_{b,n}\right)^2-\widehat{\xi}_{b,n}^{\ 4}}\right)\right\}}{\left\{\left\{d^{E_n}\breve{\vartheta}(b)\right\}\left(4-\widehat{\xi}_{b,n}^{\ 2}\right)\pm 2\widehat{\xi}_{b,n}\left\{d^{E_n}\widehat{\xi}(b)\right\}\right\}^2+\left\{2\widehat{\xi}_{b,n}^{\ 2}\left(\left\{d^{E_n}\widehat{\xi}(b)\right\}\mp\widehat{\xi}_{b,n}^{\ -1}\left\{d^{E_n}\breve{\vartheta}(b)\right\}-2\frac{\left\{d^{E_n}\breve{\vartheta}(b)\right\}\widehat{\gamma}_{d,n}^{\ 2}}{\left(\widehat{\gamma}_{d,n}\widehat{\xi}_{b,n}\right)^2-\widehat{\xi}_{b,n}^{\ 4}}\right)\right\}^2}$$

$$+ i\frac{\left\{\mp 4\widehat{\xi}_{b,n}^{\ 3}\left(\frac{1}{2}\left\{d^{E_n}\widehat{\xi}(b)\right\}\mp\frac{\widehat{\xi}_{b,n}}{4}\left\{d^{E_n}\breve{\vartheta}(b)\right\}\pm\left\{d^{E_n}\breve{\vartheta}(b)\right\}\frac{\widehat{\gamma}_{d,n}^{\ 2}\widehat{\xi}_{b,n}^{\ -1}}{\widehat{\gamma}_{d,n}^{\ 2}-\widehat{\xi}_{b,n}^{\ 2}}\right)\right\}}{\left\{\left\{d^{E_n}\breve{\vartheta}(b)\right\}\left(4-\widehat{\xi}_{b,n}^{\ 2}\right)\pm 2\widehat{\xi}_{b,n}\left\{d^{E_n}\widehat{\xi}(b)\right\}\right\}^2+\left\{2\widehat{\xi}_{b,n}^{\ 2}\left(\left\{d^{E_n}\widehat{\xi}(b)\right\}\mp\widehat{\xi}_{b,n}^{\ -1}\left\{d^{E_n}\breve{\vartheta}(b)\right\}-2\frac{\left\{d^{E_n}\breve{\vartheta}(b)\right\}\widehat{\gamma}_{d,n}^{\ 2}}{\left(\widehat{\gamma}_{d,n}\widehat{\xi}_{b,n}\right)^2-\widehat{\xi}_{b,n}^{\ 4}}\right)\right\}^2}$$

<div align="right">(B-9)</div>

iii)      Regions $L, \vec{\times}, R, \vec{\times}$ and $\vec{\times}$ contribute with two extra pole terms, (one for each sign), arising through the following condition as this is induced by eq. (23):

$$4\,\mathrm{Re}\,\breve{\vartheta}_b - \breve{\xi}_b^{\ 2}\breve{\vartheta}_b \pm \left(-4\left(\breve{\xi}_b\breve{\vartheta}_b\right)^2 + \frac{\left(4\breve{\xi}_b\widehat{\gamma}_d\right)^2\breve{\vartheta}_b\,\mathrm{Re}\,\breve{\vartheta}_b(\lambda)}{\left(4\,\mathrm{Re}\,\breve{\vartheta}_b-\breve{\xi}_b^{\ 2}\breve{\vartheta}_b\right)^2+\left(\breve{\xi}_b\widehat{\gamma}_d\right)^2}\right)^{1/2}$$

$$-(1+i)\left\{\mathrm{Re}\,\breve{\vartheta}_b + \mathrm{Im}\,\breve{\vartheta}_b\right\}\frac{1}{1+4\widehat{\delta}_a^{\ -2}} = 0 \tag{B-10}$$

We develop the above quantity around the eigenvalues $E_n$ of the unperturbed wells and impose the:

$$-i\left(\widehat{\xi}_{b,n}^{\ 2} + \frac{\widehat{\delta}_{a,n}^{\ 2}}{4}\right) \mp 2\widehat{\xi}_{b,n} - \frac{\widehat{\delta}_{a,n}^{\ 2}}{4} +$$

$$(E-E_n)\left\{\begin{array}{l}\left\{d^{E_n}\breve{\vartheta}(b)\right\}\left(-4+\widehat{\xi}_{b,n}^{\ 2}-\frac{\widehat{\delta}_{a,n}^{\ 2}}{4}\right)+2i\widehat{\xi}_{b,n}^{\ 2}\left\{d^{E_n}\widehat{\xi}(b)\right\}-\left\{d^{E_n}\widehat{\delta}(a)\right\}\frac{\widehat{\delta}_{a,n}^{\ 2}}{2}\\[2mm]\mp\widehat{\xi}_{b,n}\left(-2\left\{d^{E_n}\widehat{\xi}(b)\right\}+2i\left\{d^{E_n}\breve{\vartheta}(b)\right\}-4i\left\{d^{E_n}\breve{\vartheta}(b)\right\}\frac{\widehat{\gamma}_{d,n}^{\ 2}}{\widehat{\gamma}_{d,n}^{\ 2}-\widehat{\xi}_{b,n}^{\ 2}}\right)\\[2mm]-i\left(\frac{1}{2}\left\{d^{E_n}\breve{\vartheta}(b)\right\}+\left\{d^{E_n}\widehat{\delta}(a)\right\}\right)\frac{\widehat{\delta}_{a,n}^{\ 2}}{2}\end{array}\right\} = 0 \tag{B-11}$$

Thus, once more the perturbed eigenvalues become complex and equal to

$$Z_n^{L,\widetilde{x},R,\widetilde{x},\widetilde{x}} = E_n - \cfrac{\left[\begin{array}{l}\left(\mp 2\widehat{\xi}_{b,n} - \dfrac{\widehat{\delta}_{a,n}{}^2}{4}\right)\left\{\left\{d^{E_n}\bar{\vartheta}(b)\right\}\left(4 + \widehat{\xi}_{b,n}{}^2 - \dfrac{\widehat{\delta}_{a,n}{}^2}{4}\right) - \dfrac{\widehat{\delta}_{a,n}{}^2}{2}\left\{d^{E_n}\widehat{\delta}(a)\right\} \pm 2\widehat{\xi}_{b,n}\left\{d^{E_n}\widehat{\xi}(b)\right\}\right\} \\ + \left(-2\widehat{\xi}_{b,n}{}^2 - \dfrac{\widehat{\delta}_{a,n}{}^2}{4}\right)\left\{2\widehat{\xi}_{b,n}{}^2\left(\left\{d^{E_n}\widehat{\xi}(b)\right\} \mp \widehat{\xi}_{b,n}{}^{-1}\left\{d^{E_n}\bar{\vartheta}(b)\right\} \pm 2\left\{d^{E_n}\bar{\vartheta}(b)\right\}\dfrac{\widehat{\xi}_{b,n}{}^{-1}\widehat{\gamma}_{d,n}{}^2}{\widehat{\gamma}_{d,n}{}^2 - \widehat{\xi}_{b,n}{}^2}\right) - \dfrac{\widehat{\delta}_{a,n}{}^2}{2}\left(\dfrac{1}{2}\left\{d^{E_n}\bar{\vartheta}(b)\right\} + \left\{d^{E_n}\widehat{\delta}(a)\right\}\right)\right\}\end{array}\right]}{\left[\begin{array}{l}\left\{\left\{d^{E_n}\bar{\vartheta}(b)\right\}\left(-4 + \widehat{\xi}_{b,n}{}^2 - \dfrac{\widehat{\delta}_{a,n}{}^2}{4}\right) \pm 2\widehat{\xi}_{b,n}\left\{d^{E_n}\widehat{\xi}(b)\right\} - \dfrac{\widehat{\delta}_{a,n}{}^2}{2}\left\{d^{E_n}\widehat{\delta}(a)\right\}\right\}^2 + \\ \left\{2\widehat{\xi}_{b,n}{}^2\left(\left\{d^{E_n}\widehat{\xi}(b)\right\} \mp \widehat{\xi}_{b,n}{}^{-1}\left\{d^{E_n}\bar{\vartheta}(b)\right\} \pm 2\left\{d^{E_n}\bar{\vartheta}(b)\right\}\dfrac{\widehat{\xi}_{b,n}{}^{-1}\widehat{\gamma}_{d,n}{}^2}{\widehat{\gamma}_{d,n}{}^2 - \widehat{\xi}_{b,n}{}^2}\right) - \dfrac{\widehat{\delta}_{a,n}{}^2}{2}\left(\dfrac{1}{2}\left\{d^{E_n}\bar{\vartheta}(b)\right\} + \left\{d^{E_n}\widehat{\delta}(a)\right\}\right)\right\}^2\end{array}\right]}$$

$$+ i\cfrac{\left[\begin{array}{l}\left(\mp 2e^{-\phi(\lambda_n)} - \dfrac{e^{-2\delta_a(\kappa)}}{4}\right)\left\{2e^{-2\phi_a(\lambda)}\left(\left\{d^{E_n}\widehat{\xi}(b)\right\} \mp e^{\phi_a(\lambda)}\left\{d^{E_n}\bar{\vartheta}(b)\right\} \pm 2\left\{d^{E_n}\bar{\vartheta}(b)\right\}\dfrac{e^{-2\gamma_n(\nu)+\phi_a(\lambda)}}{e^{-2\gamma_n(\nu)} - e^{-2\phi_a(\lambda)}}\right) - \dfrac{\widehat{\delta}_{a,n}{}^2}{2}\left(\dfrac{1}{2}\left\{d^{E_n}\bar{\vartheta}(b)\right\} + \left\{d^{E_n}\widehat{\delta}(a)\right\}\right)\right\} + \\ \left(e^{-\phi(\lambda_n)} + \dfrac{\widehat{\delta}_{a,n}{}^2}{4}\right)\left\{\left\{d^{E_n}\bar{\vartheta}(b)\right\}\left(-4 + \widehat{\xi}_{b,n}{}^2 - \dfrac{\widehat{\delta}_{a,n}{}^2}{4}\right) \pm 2e^{-\phi_a(\lambda)}\left\{d^{E_n}\widehat{\xi}(b)\right\} - \dfrac{\widehat{\delta}_{a,n}{}^2}{2}\left\{d^{E_n}\widehat{\delta}(a)\right\}\right\}\end{array}\right]}{\left[\begin{array}{l}\left\{\left\{d^{E_n}\bar{\vartheta}(b)\right\}\left(-4 + \widehat{\xi}_{b,n}{}^2 - \dfrac{\widehat{\delta}_{a,n}{}^2}{4}\right) \pm 2\widehat{\xi}_{b,n}\left\{d^{E_n}\widehat{\xi}(b)\right\} - \dfrac{\widehat{\delta}_{a,n}{}^2}{2}\left\{d^{E_n}\widehat{\delta}(a)\right\}\right\}^2 + \\ \left\{2\widehat{\xi}_{b,n}{}^2\left(\left\{d^{E_n}\widehat{\xi}(b)\right\} \mp \widehat{\xi}_{b,n}{}^{-1}\left\{d^{E_n}\bar{\vartheta}(b)\right\} \pm 2\left\{d^{E_n}\bar{\vartheta}(b)\right\}\dfrac{\widehat{\xi}_{b,n}{}^{-1}\widehat{\gamma}_{d,n}{}^2}{\widehat{\gamma}_{d,n}{}^2 - \widehat{\xi}_{b,n}{}^2}\right) - \dfrac{\widehat{\delta}_{a,n}{}^2}{2}\left(\dfrac{1}{2}\left\{d^{E_n}\bar{\vartheta}(b)\right\} + \left\{d^{E_n}\widehat{\delta}(a)\right\}\right)\right\}^2\end{array}\right]}$$

(B-12)

# REFERENCES

[1] N. S. Yanofsky and M.A. Mannucci, Quantum Computing, Cambridge: Cambridge University Press, 2008, pp. 138-142.

[2] T. Hey, Comput. Control Eng. J., 10(3), 105, (1999).

[3] E. Rieffel and W. Polak, ACM Comput. Surv., 32(3), 300, (2000).

[4] M. Russ and G. Burkard, J. Phys. Condensed Matter, 29(39), 393001, (2017).

[5] X.-Y. Zhu, T. Tu, A.-L. Guo, Z.-Q. Zhou, C.-F. Li, and G.-C. Guo, Sci. Rep., 8(1), 15761, (2018).

[6] T. Fujisawa, T. Hayashi, H. D. Cheong, Y. H. Jeong, and Y. Hirayama, Phys. E, Low-Dimensional Syst. Nanostruct., 21(2) 1052, (2004).

[7] A. Weichselbaum and S. Ulloa, Phys. Rev. A, Gen. Phys., 70(3), 032328, (2004).

[8] D. P. K. Bladh and T. Duty, *New J. Phys.*, 7(1), 180, (2005).

[9] M. Lutchyn, .. Cywiski, C. P. Nave, and S. Das Sarma, Phys. Rev. B, Condens. Matter, 78(2), 024508, (2008).

[10] M. Gonzalez-Zalba. (2018). ``Solid state qubits." [Online]. Available: https://arxiv.org/abs/1801.06722

[11] T. Stievater *et al*., Phys. Rev. Lett., 87(13), 133603, (2001).

[12] S. Datta, Quantum Transport: Atom to Transistor. Cambridge, U.K.: Cambridge Univ. Press, 2005, pp. 47-52.

[13] C.H. Townes, and A.L. Schawlow, Microwave Spectroscopy, New York: Dover Publications, 1975, pp. 300-307.

[14] R.P. Feynman, R.B. Leighton, and M. Sands, The Feynman Lectures on Physics, Volume III, Massachusset: Addison-Wesley, Reading, 1963, pp. 115-129.

[15] G.J. Milburn, J. Corney, E.M. Wright and D.F. Walls, Physical Review A, 55(6), 4318, (1997).

[16] Y. Shin, M. Saba, T.A. Pasquini, W. Ketterle, D.E. Pritchard and A.E. Leanhardt, Phys. Rev. Lett., 92(5), 050405, (2004).

[17] D. Dast, D. Haag, H. Cartarius, G. Wunner, R. Eichler and J. Main, Fortschritte der Physik, 61(2-3), 124-139, (2013).

[18] J.L. Baudour, H.T. Cailleau and W.B. Yelon, Acta Crystallographica Section B: Structural Crystallography and Crystal Chemistry, 33(6), 1773-1780, (1977).

[19] T. Schumm, S. Hofferberth, L.M. Andersson, S. Wildermuth, S. Groth, I. Bar-Joseph, .., ... and P. Krüger, Nature Physics, 1(1), 57-62, (2005).

[20] A. Landau, Y. Aharonov and E. Cohen, International Journal of Quantum Information, 14(05), 1650029, (2016).

[21] L. Pezzé, A. Smerzi, G.P. Berman, A.R. Bishop and L.A. Collins, Physical Review A, 74(3), 033610, (2006).

[22] I. L. Chuang and Y. Yamamoto, Phys. Rev. A 52, 3489, (1995); Phys. Rev. Lett. 76, 4281 (1996).

[23] Y. Aharonov, E. Cohen, A. Landau and A. Elitzur, Scientific reports, 7(1), 1-9, (2017)

[24] M. Lodari, A. Tosato, D. Sabbagh, M.A. Schubert, G.Capellini, A. Sammak, A., ... & G. Scappucci, G., Physical Review B, 100(4), 041304, (2019).

[25] C. Adami and N. J. Cerf, Quantum computation with linear optics. In NASA International Conference on Quantum Computing and Quantum Communications (pp. 391-401). Springer, Berlin, Heidelberg, (1998).

[26] X.Q. Li, and Y. Arakawa, Y. (2000). Phys. Rev. A, 63(1), 012302, (2000).

[27] J. Gorman, D.G. Hasko, and D.A. Williams, Phys. Rev. Lett. 95(9), 090502, (2005).

[28] P. Giounanlis, E. Blokhina, K. Pomorski, D.R. Leipold, and R.B. Staszewski, IEEE Access, 7, 49262, 92019).

[29] T.P. Orlando, S. Lloyd, L.S. Levitov, K.K. Berggren, M.J. Feldman, M.F., Bocko, and C.H. Van der Wal, Physica C: 'Superconductivity, 372,194, (2002).

[30] R.H. Koch, G.A. Keefe, F.P. Milliken, J.R. Rozen, C.C. Tsuei, J.R. Kirtley, and D.P. DiVincenzo, Phys. Rev. Lett. 96(12), 127001, (2006).

[31] M.G. Castellano, F. Chiarello, P. Carelli, C. Cosmelli, F. Mattioli and G. TorrioliNew Journal of Physics, 12(4), 043047, (2010).

[32] R. Malek, and K.P. Wanczek, Rapid communications in mass spectrometry, 11(14), 1616-1618, (1997).

[33] A. Retzker, R.C. Thompson, D.M. Segal, and M.B. PlenioPhys. Rev. Lett. 101(26), 260504, (2008).

[34] N. Friis, O. Marty, C. Maier, C. Hempel, M. Holzäpfel, P. Jurcevic and B. Lanyon, Physical Review X, 8(2), 021012, (2018).

[35] C.J. Foot and M.D. Shotter, Am. J. Phys., 79(7), 762(2011).

[36] W. Dür and S. Heusler, "What we can learn about quantum physics from a single qubit." arXiv preprint arXiv:1312.1463 (2013).

[37] A. Landau, Y. Aharonov, and E. Cohen, Int. J. Quant. Inf., 14(05), 1650029(2016).

[38] M.D. Kim, D. Shin, and J. Hong, J. Phys. Rev. B, 68(13), 134513, (2003).

[39] Y. V. Fominov,A.A. Golubov, and M.Y. Kupriyanov, Journal of Experimental and Theoretical Phys. Lett, 77(10), 587, (2003).

[40] P.D. Shaju, , V. C. Kuriakose Physica C, 424(3), 125(2005).

[41] R.J. Monaco, Phys. C, 28(44), 445702, (2016).

[42] S. Savel'ev, X. Hu and F. Nori, New J. Phys., 8(6), 105, (2006).

[43]  K.M. Indlekofer, T. Schäpers, T. On the Possibility of Using Semiconductor Nanocolumns for the Realization of Quantum Bits. arXiv preprint cond-mat/0703520, (2007).

[44] V. Ivády, J. Davidsson, N. Delegan, A.L. Falk, P. V.  Klimov, S.J. Whiteley, and A. Gali, Nature communications, 10(1), 1-8, (2019).

[45] J.C. Abadillo-Uriel, M.J. Calderón, New J. Phys., 19(4), 043027, (2017).

[46] P. Jakubczyk, K. Majchrowski, I. Tralle, Acta Physica Polonica A, 132(1), 115(2017).

[47] N.W. Hendrickx, D.P. Franke, A. Sammak, G. Scappucci and M. Veldhorst, Nature, 577(7791), 487, (2020).

[48] D. Loss and D. P. DiVincenzo. Phys. Rev. A, 57(1), 120, (1998).

[49] J.A. Schreier, A. A. Houck,J. Koch, D.I. Schuster, B.R. Johnson, J.M. Chow,  ... and R.J. Schoelkopf, Phys. Rev. B, 77(18), 180502, (2008).

[50]  T.G. Douvropoulos and C.A. Nicolaides,  J. Chem. Phys., 119, 8235, (2003).

[51]  T.G. Douvropoulos and C.A. Nicolaides,  I. J. Quant. Chem.,106, 1032, (2006).

[52] E. Merzbacher, Quantum Mechanics, New York: John Wiley, 1998, pp.320-326.

[53] R.P. Feynman and A.R. Hibbs, Quantum Mechanics and Path Integrals, New York: McGraw-Hill, 1965, pp. 31-39.

[54]  M. Razavy, Quantum Theory of Tunneling, New Jersey: World Scientific, 2003, pp. 219-220.

[55]  M.C. Gutzwiller, J. Math. Phys.,12 , 343, (1971).

[56] W.H.  Miller, J. Chem. Phys., 56 , 38, (1972).

[57] W.H.  Miller and T.F. George, J. Chem. Phys. 56 , 5668, (1972).

[58]  B.R. Holstein and A.R. Swift, Am. J. Phys.  50, 829, (1982).

[59]  H. Kleinert, Path Integrals, New Jersey: World Scientific, 1995, pp. 199-226.

[60]  L.D. Landau and E.M. Lifshitz, Quantum Mechanics, 2nd ed., Oxford: Pergamon Press, 1965, pp. 183-184.

[61]  C.C. Gerry and P.L. Knight, Introductory Quantum Optics, Cambridge: Cambridge University Press, 2005, pp. 90-93.

[62]  S. Flugge, Practical Quantum Mechanics, Berlin Heidelberg: Springer-Verlag, 1999, pp. 365-368.

[63]  T.G. Douvropoulos and C.A. Nicolaides, Phys. Rev.  A, 69, 032105, (2004).

[64] C.J. Myatt, B.E. King, Q.A. Turchette, C.A. Sackett, D. Kielpinski, W.M. Itano,  ... & D.J. Wineland, Nature, 403(6767), 269, (2000).

[65]  S. Sarkar, S. Paul, C. Vishwakarma, S. Kumar, G.Verma, M. Sainath, ... & M.S. Santhanam, Phys. Rev. Lett. 118(17), 174101, (2017).

[66] L.F. Qiao, A. Streltsov, J. Gao, S. Rana, R.J. Ren, Z.Q. Jiao, ... & X.M. Jin Phys. Rev. A, 98(5), 052351, (2018).